HEALTH AND MEDICINE

A highly selective JAK3 inhibitor is developed for treating rheumatoid arthritis by suppressing γc cytokine–related JAK-STAT signal

Chengjuan Chen[1], Yuan Yin[2], Gaona Shi[1], Yu Zhou[1], Shuai Shao[1], Yazi Wei[1], Lei Wu[1], Dayong Zhang[2]*, Lan Sun[1]*, Tiantai Zhang[1]*

Janus kinases (JAKs) play a critical role in immune responses by relaying signals from more than 50 cytokines, making them attractive therapeutic targets for autoimmune diseases. Although approved JAK inhibitors have demonstrated clinical efficacy, they target a broad spectrum of cytokines, which results in side effects. Therefore, next-generation inhibitors maintain efficacy, while sparing adverse events need to be developed. Among members of the JAK family, JAK3 only regulates a narrow spectrum of γc cytokines and becomes a potentially ideal target. Here, a highly JAK3-selective inhibitor Z583 is developed, which showed a potent inhibition of JAK3 with an IC_{50} of 0.1 nM and exhibited a 4500-fold selectivity for JAK3 than other JAK subtypes. Furthermore, Z583 completely inhibited the γc cytokine signaling and sufficiently blocked the development of inflammatory response in RA model, while sparing hematopoiesis. Collectively, the highly selective JAK3 inhibitor Z583 is a promising candidate with significant therapeutic potential for autoimmune diseases.

INTRODUCTION

Rheumatoid arthritis (RA) is a chronic systemic autoimmune disease that is characterized by progressive synovial inflammation of joints, as well as irreversible cartilage damage and bone erosion. This results in physical dysfunction and disability of multiple joints (*1*, *2*). Over the past three decades, disease-modifying antirheumatic drugs (DMARDs), which have been shown to reduce inflammation, relieve pain, and delay joint destruction, have been the mainstay of RA treatment (*3*). Methotrexate (MTX) is the most widely applied drug in RA management in pharmacological research and clinical practice as the first-line anchored DMARD (*4*, *5*). Subsequently, with the advent of newer biological DMARDs (bDMARDs), "biologic therapies" of inhibiting inflammatory factors by monoclonal antibody offer a novel opportunity and have been an important advancement in the treatment of RA (*6*, *7*). However, the severe systemic complications caused by long-term use of MTX and the potential immunogenicity of bDMARDs are limitations in clinical application (*8*, *9*). Furthermore, the current DMARDs have almost no positive effect with regard to cartilage and bone destruction in RA treatment. Therefore, it is crucial to develop more effective and safer drugs against RA.

With the approval of tofacitinib via the U.S. Food and Drug Administration for the treatment of RA in 2012, the Janus kinase (JAK) family has been validated as a new and effective therapeutic target in inflammatory and autoimmune diseases (*10*). The JAK family non–receptor protein–associated tyrosine kinases, including JAK1, JAK2, JAK3, and tyrosine kinase 2 (TYK2), relay signals downstream of type I and type II cytokine receptors through signal transducers and activators of transcription (STATs) (*11*). The JAK-STAT signaling pathway is now recognized as an evolutionarily conserved signaling pathway in innate immunity, inflammation, and hematopoiesis, and disorders frequently appear in cancers and autoimmune and inflammatory diseases (*12*, *13*). More than 50 cytokines, including interleukins (ILs), interferons (IFNs), colony-stimulating factors (CSFs), growth factors, and hormones, are dependent on the JAK-STAT signaling pathway to mediate cellular proliferation, differentiation, survival, and immune response (*14*, *15*). JAK-dependent cytokines are critical regulators of immunity and inflammation and have been shown to contribute to the immunopathology that underlies inflammatory and autoimmune diseases, such as RA (*16*). The relationship between JAKs and different diseases has been revealed by functional mutation and polymorphisms of JAKs in cells, mice, or human (*17*, *18*). Therefore, targeting JAKs to prevent its phosphorylation can inhibit the inflammatory response that is induced by overexpression of cytokines. These rational and solid evidences indicate that JAKs are ideal therapeutic target for inflammatory and autoimmune diseases.

To date, eight JAK inhibitors (JAKinibs) have been granted approval by various regulatory agencies for the treatment of many diseases, including myeloproliferative neoplasms (ruxolitinib by Incyte and Novartis and fedratinib by Sanofi) and inflammatory and autoimmune diseases (tofacitinib by Pfizer, baricitinib by Incyte and Lilly, peficitinib by Astellas Pharma, upadacitinib by AbbVie, delgocitinib by Torii Pharmaceutical, and filgotinib by Gilead) (*19*). Among them, tofacitinib, baricitinib, peficitinib, and delgocitinib are first-generation pan-JAKinibs that nonselectively inhibit multiple subtypes of JAKs and target a broad spectrum of cytokines (*20*). Although inappropriate or excessive production of cytokines is known to be the cause of inflammatory and autoimmune diseases, widespread suppression of cytokines also limits normal biological functions. For instance, hematopoietic growth factors, such as erythropoietin (EPO) and thrombopoietin (TPO) regulate erythropoiesis, myelopoiesis, and inflammation via the JAK2 subtype, and their blockade can cause severe adverse effects (*21*). Therefore, it is not unexpected that the side effects of pan-JAKinibs are predictable on the basis of their biological functions as signal transducers for a large number of cytokines, which include infection, hematological and cardiovascular

[1]State Key Laboratory of Bioactive Substance and Function of Natural Medicines, Institute of Materia Medica, Chinese Academy of Medical Sciences and Peking Union Medical College, Beijing 100050, China. [2]School of Science, China Pharmaceutical University, Nanjing 210009, China.
*Corresponding author. Email: ttzhang@imm.ac.cn (T.Z.); sunhanxing2005@imm.ac.cn (L.S.); cpuzdy@163.com (D.Z.)

event, hyperlipidaemia, and cancer (*20*). Given the adverse events of broad-spectrum cytokine targeting by first-generation JAKinibs, the development of the next-generation JAKinibs with more selectivity for the subtype of JAKs may be an optimizing strategy. Although upadacitinib and filgotinib have been developed as next-generation potent selective JAK1 inhibitors, biochemical assays have demonstrated that their selectivity is not ideal, with 2.4- and 2.8-fold preference for JAK1 over JAK2, respectively (*22*, *23*). Ritlecitinib is the most advanced selective JAK3 inhibitor developed by Pfizer with a median inhibitory concentration (IC_{50}) of 33.1 nM for JAK3 [1 mM adenosine triphosphate (ATP)] and displayed no activity against the other JAK isoforms (>10,000 nM against JAK1, JAK2, and TYK2) (*24*). It is currently in phase 2b/3 clinical trial (NCT03732807) in alopecia areata as a dual JAK3/tyrosine protein kinase (TEC) family kinase inhibitor (*25*). Therefore, to date, no truly selective JAKinibs have been approved for the market.

Here, we developed a newly irreversible covalent JAK3-selective inhibitor Z583 with an IC_{50} value of 0.1 nM [Michaelis constant (K_m) ATP] or 10.84 nM (1 mM ATP), which exhibits excellent anti-RA effect by suppressing the activation of the JAK-STAT pathway by binding to the cysteine residue at position 909 (Cys^{909}) in the JAK3 subtype. We also validated that the Z583 intervention blocked the progression of collagen-induced arthritis (CIA) in a mouse model. Thus, Z583 may represent a highly promising candidate for the treatment of autoimmune or inflammatory diseases and warrants clinical investigation.

RESULTS

Z583 is identified as a potently selective inhibitor of JAK3

On the basis of the structural difference of amino acid residue at the 909 position between JAK3 and other JAK isoforms, compounds were designed to target Cys^{909} ATP binding pocket of JAK3 isoform. A series of targeted synthetic compounds were screened for the inhibitory activity against four members of JAK kinase using homogenous time-resolved fluorescence (HTRF) assay. The primary screening results were analyzed and used to design new compounds for structural optimization. After several rounds of screening, a class of active compounds with inhibitory activity IC_{50} < 10 nM for JAK3 subtype and selectivity of >100-fold against the other JAK isoforms were selected to further evaluate the effects on JAK-STAT signaling pathway at the cellular level. Following extensive screening and evaluation showed that Z583, a novel lead compound, exhibited good potency and selectivity for inhibiting the phosphorylation of JAK3 (Fig. 1A). The results indicated that Z583 had a potent inhibitory activity for JAK3 with an IC_{50} value of 0.1 nM in the presence of 1.43 μM (K_m) ATP and IC_{50} value of 10.84 nM at 1 mM ATP concentration. Among the JAK family subtypes, Z583 displayed a remarkable selectivity of >920-fold for JAK3 over the other JAK isoforms (IC_{50} > 10,000 nM against JAK1, JAK2, and TYK2) at 1 mM ATP concentration (Fig. 1B). Our findings also demonstrated that Z583 had advantage over ritlecitinib in activity and selectivity for JAK3 at the same concentration of ATP (1 mM) in free-cell assays (Fig 1C). To further understand the kinome profiling of Z583, we assessed it against a panel of 463 human kinases (400 wild-type and 63 mutant) in the KINOMEscan Assay Platform (DiscoverX) using an in vitro ATP site competition binding assay at 0.1 μM concentration (table S1). Z583 exhibited excellent binding affinity for JAK3 with a selectivity score of 0.01 (Fig. 1D). However, it also showed affinity to several other kinases, including the TEC family, which may cause potential off target effects in clinical applications. Nevertheless, since the kinome profiling assay can only reveal the affinity of Z583 with kinases and not their inhibitory functions, we next tested the inhibitory effect of Z583 (0.1 μM) against a panel of 48 kinases (K_m ATP) using a Z′-LYTE kinase binding assay. The results indicated that only four kinases, each with a cysteine residue at a position comparable to that of Cys^{909} in JAK3, exhibited >80% inhibition (Fig. 1E). Furthermore, the kinases with the cysteine residue and the JAK family were selected to evaluate the intensity of inhibition by Z583. The IC_{50} value of Z583 against JAK3 was 0.1 nM, as opposed to 2.91, 3.18, and 4.42 nM against the TEC family kinases TXK, BMX, and BTK, respectively (Fig. 1F). These results indicate a 30-fold higher selectivity to JAK3. Together, Z583 is a selective and potent inhibitor of the JAK3 subtype.

Z583 covalently binds to Cys^{909} and irreversibly inhibits JAK3 subtype

Z583 had remarkable potency and outstanding selectivity for the JAK3 isoform within JAK family of kinases. To further evaluate the target engagement and binding mode of Z583 with the JAK3 protein [Protein Data Bank (PDB): 4Z16], we conducted a molecular docking study. Our in silico results revealed that the electrophilic carbon of Z583 can form a covalent bond with Cys^{909} through the Michael addition reaction (Fig. 2A). The pyrazolopyrimidine ring scaffold fits well into the JAK3 ATP binding pocket and forms a hydrogen bond with atoms of Leu^{905}. In addition, the amide group and methoxyethyl side chain formed a hydrogen bond with Leu^{828}, Val^{836}, Ala^{853}, Try^{904}, and Leu^{956}, respectively. To confirm the bona fide covalent interaction of Z583 with the JAK3 protein, we carried out a cell-based "washout" experiment to determine the effects of Z583 on STAT5, which is an effector of JAK3 downstream signaling. Z583 persistently inhibited the expression of phosphorylated STAT5 (p-STAT5) induced by γ chain (γc) cytokines of IL-2 or IL-15 in $CD4^+$ T cells from C57BL/6, even after washout of the supernatant (Fig. 2B). These data suggest that the binding of Z583 with JAK3 is likely a type of covalent and irreversible manner. On the basis of the hints of covalent and irreversible bond of Z583 with JAK3 protein by molecule docking study and cellular assay, mass spectrometry was used to confirm the binding site between Z583 and JAK3. After incubating Z583 with a recombinant JAK3 kinase domain, the digested complex by protease was then subjected to a mass spectrometry experiment. Liquid chromatography–tandem mass spectroscopy (LC-MS/MS) analysis identified a peptide of LVMEYLPSGC*LR, wherein the C* corresponds to the Cys^{909} residues that were modified by Z583 (Fig. 2C) in agreement with the above molecule docking and cell-based experiments. Together, these cumulative data provide manifold and strong evidence to confirm that Z583 covalently binds to Cys^{909} residue and irreversibly inhibits JAK3 kinase.

Z583 selectively inhibited JAK3-dependent common γc cytokine signaling

Each JAK subtype has a specific response for a different set of cytokine receptors, which is bound by the corresponding cytokines to contribute the function through JAK protein. Conventionally, JAKs relay signals in the form of heterodimers (i.e., JAK1/JAK3) or homodimers (such as JAK2/JAK2) (Fig. 3A). The JAK3 subtype is restricted to expression in hematopoietic cells and is exclusively associated with only the common γc receptor subunit of IL-2, IL-4,

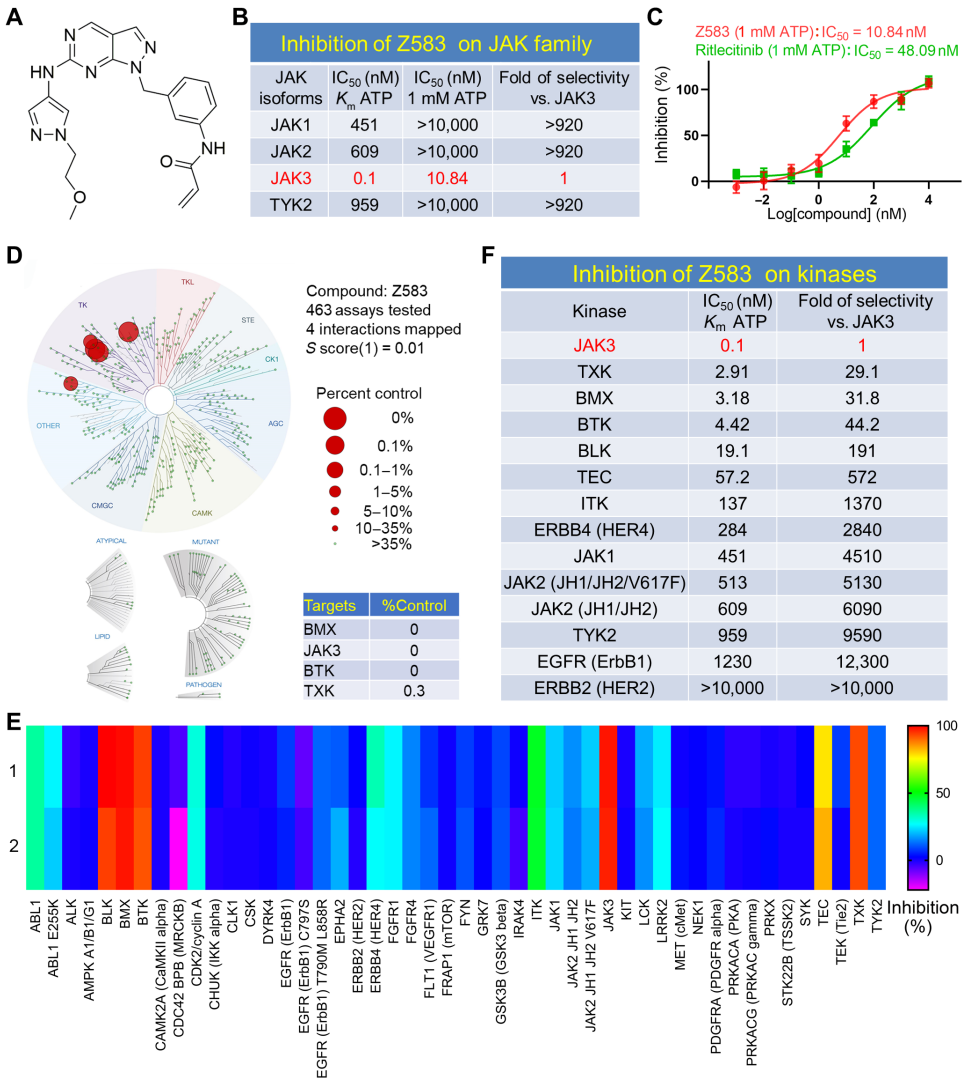

Fig. 1. The biological characteristics of selective JAK3 inhibitor Z583. (**A**) The structure of compound Z583. (**B**) Inhibitory activity and selectivity of Z583 for JAK family kinases at K_m ATP and 1 mM ATP concentration. (**C**) The IC_{50} of Z583 and ritlecitinib inhibiting JAK3 at 1 mM ATP concentration. (**D**) KINOMEscan kinase selectivity profile for Z583 at a concentration of 0.1 μM. (**E**) The selective inhibition of Z583 against a panel of 48 kinases. (**F**) The inhibitory potent and selectivity of Z583 for JAK family kinases and kinases with cysteine residue.

IL-7, IL-9, IL-15, and IL-21, which are integral to lymphocyte activation, function, and proliferation. To further understand the selective inhibitory effects of Z583 among different JAK isoforms, we stimulated human peripheral blood mononuclear cells (hPBMCs) with multiple cytokines or human $CD34^+$ cells with EPO and measured the phosphorylation levels of the cognate STATs. For instance, JAK3 inhibition was evaluated by measuring the expression of p-STAT5 (IL-2, IL-7, IL-9, IL-15, and IL-21) or p-STAT6 (IL-4), JAK2 inhibition through p-STAT5 (EPO) or p-STAT5 [granulocyte-macrophage CSF (GM-CSF)], and JAK1/JAK2/Tyk2 inhibition through the IL-6–stimulated STAT3 phosphorylation. STAT1 phosphorylation was evaluated to assess the JAK1/Tyk2, JAK2/Tyk2, or JAK1/JAK2 inhibition in response to IL-10, IL-13, or IFN-γ, respectively (Fig. 3B). Our data demonstrate that Z583 almost completely inhibited the γc cytokine–stimulated phosphorylation of STAT5 (by IL-2, IL-7, IL-9, IL-15, and IL-21) and STAT6 (by IL-4) (Fig. 3, C and E). On the other hand, Z583 did not inhibit STAT phosphorylation induced by non–JAK3-associated cytokines (Fig. 3, D and F). These results demonstrate that Z583 blocks cytokine signaling via the JAK3 subtype but not through other JAK family isoforms. In addition, to understand the difference in activity and selectivity of Z583 and ritlecitinib for JAK3 or other JAK members in multiple cytokine signaling pathways, we compared their effects on p-STAT levels by multiple cytokine stimulation. The results indicated that they all showed potent inhibition for γc cytokine (IL-2)–induced p-STAT5 levels but not p-STAT3, p-STAT1, and p-STAT5 induced by non–γc cytokine of IL-6, IL-10, and GM-CSF, respectively (fig. S1, A to D).

Z583 inhibited the maturation of dendritic cells in vitro

Dendritic cells (DCs) are central in initiating the adaptive immune response and in mediating immune tolerance across autoimmune and inflammatory diseases. During the progression of RA, mature DCs (mDCs) play a key role in the induction and amplification of the immune response by presenting self-antigens or secreting cytokines

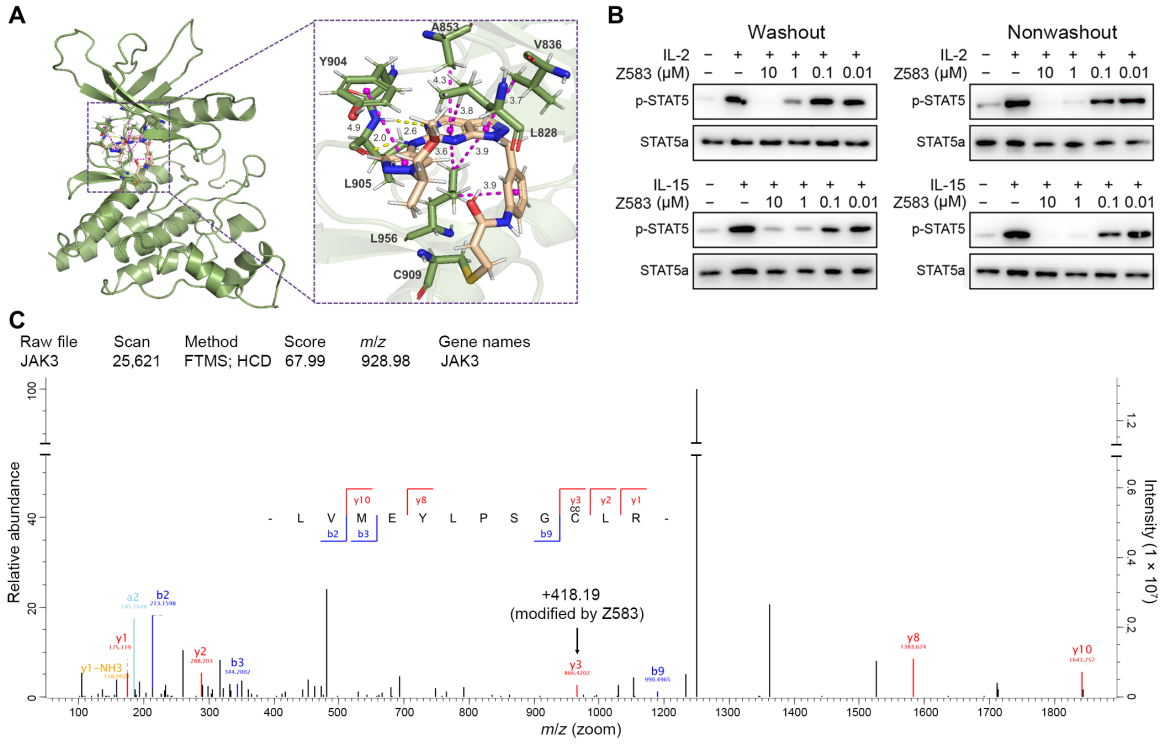

Fig. 2. The binding property of Z583 with JAK3 subtype. (**A**) Z583 can bind to Cys^{909} of the x-ray crystal of JAK3 (PDB ID: 4Z16). (**B**) Z583 irreversibly inhibits the expression of p-STAT5 after stimulation by γc cytokines of IL-2 or IL-15 in $CD4^+$ T cells from C57BL/6, even after being washed extensively with phosphate-buffered saline. (**C**) LC-MS/MS experiments identified a single modified peptide LVMEYLPSGC*LR (C*, cysteine residue) by Z583 at Cys^{909} position. *m/z*, mass/charge ratio.

to activate naïve T cells, which differentiate into the T helper (T_H) subtypes, including T_H1 or T_H17 cells. To assess the effect of Z583 on the maturation of DCs, monocytes that are isolated from the bone marrow of C57BL/6 mice were cultured in vitro in the presence of lipopolysaccharide (LPS). After 24 hours of LPS stimulation, the $CD11c^+$ DCs displayed obvious protrusions, which are indicative of maturation. However, Z583 prevented the transformation of immature DCs (iDCs) into mDCs in a concentration-dependent manner under a microscope (Fig. 4A). The mDCs directly mediate the activation of T cells via the costimulatory molecules CD86 and CD80. Our results demonstrated that the Z583-treated DCs ($CD11c^+$) express significantly lower levels of CD80 and CD86 in a concentration-dependent manner compared to untreated mDCs (Fig. 4, B and C). Since DCs regulate immune responses by secreting cytokines, we next measured the levels of different cytokines in the supernatant of stimulated DCs. High levels of tumor necrosis factor–α (TNF-α), IL-6, and IL-12 were prevented by Z583 in the supernatant of LPS-treated mDCs compared to that of untreated control mDCs (Fig. 4, D to F). Together, selective inhibition by Z583 prevented the maturation of LPS-stimulated DCs.

Z583 inhibited T_H1 and T_H17 cell proliferation and differentiation

The proliferation and differentiation of $CD4^+$ T cells into functionally distinct subsets of T_H cells are critical to clear specific pathogens and are also involved in the development of autoimmune diseases. The γc-dependent cytokines contribute to T_H cell differentiation into the T_H1 (IL-2) and T_H17 (IL-21) subsets through the JAK-STAT signaling pathway (*26*, *27*). Therefore, we analyzed the effect of Z583 on the proliferation and differentiation of naïve T cells. Briefly, naïve $CD4^+$ T cells were isolated from the lymph nodes of C57BL/6 mice and stimulated with anti-CD3/anti-CD28 in the presence or absence of Z583 for 72 hours. Z583 significantly inhibited anti-CD3/CD28–induced proliferation of T cells (Fig. 5A). Since the IFN-γ–producing T_H1 cells and IL-17A–producing T_H17 cells were responsible for RA development in mice and humans, we next determined whether Z583 also has an effect on T_H1 and T_H17 differentiation. Z583 significantly inhibited the differentiation of naïve $CD4^+$ T cells into T_H1 cells in a concentration-dependent manner, as demonstrated by decreased IFN-γ production (Fig. 5, B and C). In addition, Z583 also suppressed the differentiation of naïve $CD4^+$ T cells to T_H17 cells under the T_H17-polarizing conditions in vitro by abolishing IL-17A production (Fig. 5, D and E). Together, JAK3 inhibition by Z583 diminishes T cell proliferation, differentiation, and function in vivo and in vitro.

Z583 treatment alleviated CIA in mice

To evaluate the therapeutic potential of Z583 against RA, the autoimmune CIA model in DBA/1 mice was used to evaluate the effect of Z583 on the development of inflammatory phenotype in vivo. The arthritic mice were treated with three doses of Z583 (3, 1, and 0.3 mg/kg) by oral administration over a period of 3 weeks to confirm the therapeutic effect after treatment on day 27 (Fig. 6A). Consistent with the macroscopic evidences of hind paws (Fig. 6B), Z583 (3 mg/kg) almost completely prevented arthritic progression compared to vehicle-treated mice, which was also corroborated with regard to the clinical score and arthritis incidence (Fig. 6, C and D). Histopathological analysis and three-dimensional (3D) micro–computed

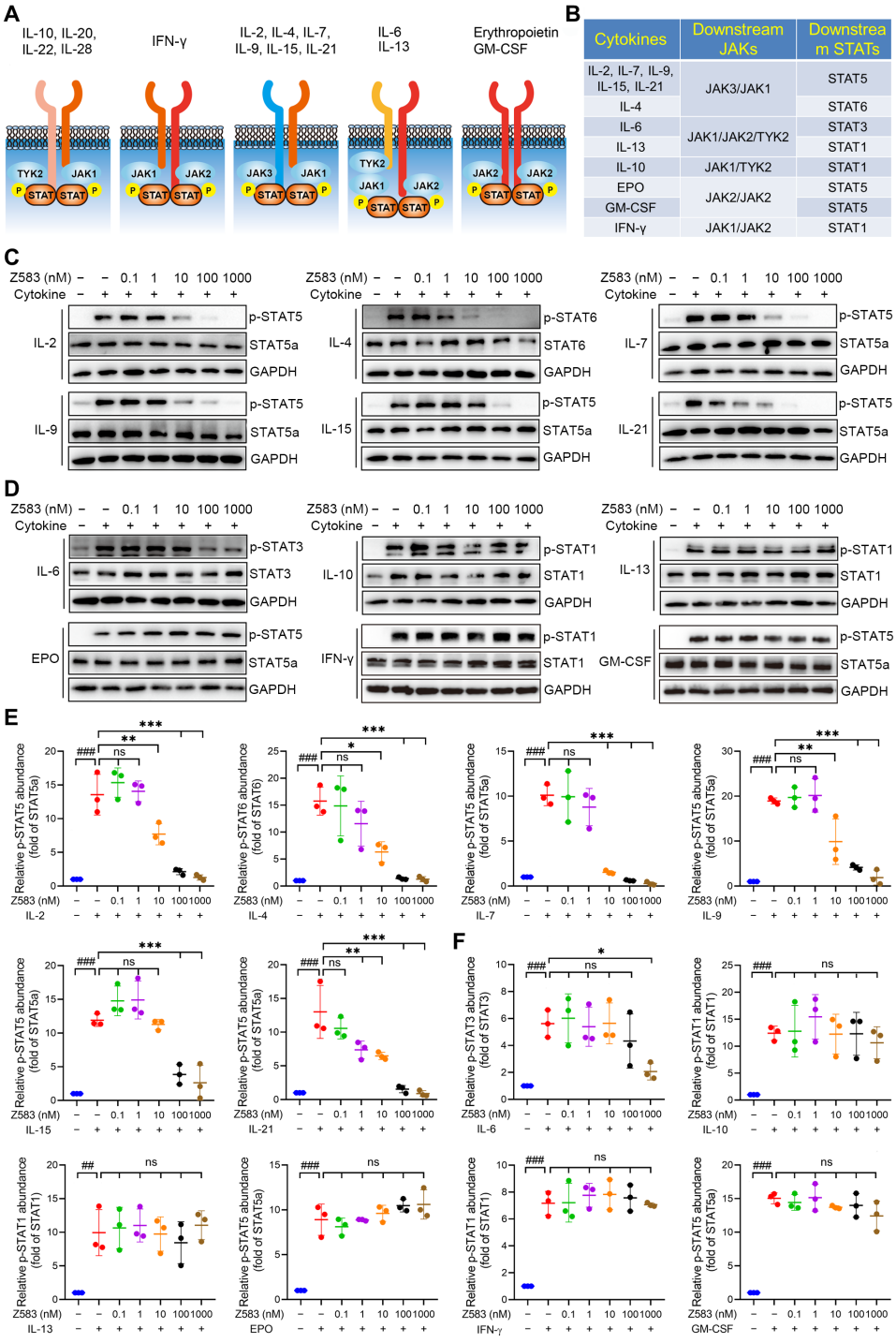

Fig. 3. Z583 selectively inhibited the JAK3-dependent signaling pathway in hPBMCs. (**A**) Four JAK subtypes (JAK1, JAK2, JAK3, and Tyk2) relay intracellular signal transduction with combinations of heterodimers or homodimers. (**B**) JAKs and STATs engage associated cytokines to mediate biological function. hPBMCs or $CD34^+$ cells (for EPO) with or without various concentrations of Z583 were stimulated with JAK3-particular γc cytokines (**C** and **E**) or other cytokines (**D** and **F**). Western blots were carried out to evaluate the expression of cytokine-associated STAT phosphorylation. All data are from three independent experiments. Data are presented as means ± SEM. ##$P < 0.01$, ###$P < 0.001$ versus control group and *$P < 0.05$, **$P < 0.01$, and ***$P < 0.001$ versus alone cytokine-stimulating group. ns, no statistical significance.

tomography (micro-CT) imaging of the joints were carried out at the end of the experiment to assess the effect of Z583 on inflammation and bone injury (Fig. 6, E and I). The joints of vehicle-treated CIA mice demonstrated a massive influx of inflammatory cells, synovial proliferation and pannus formation, cartilage damage, and bone degradation. However, 3 weeks of Z583 treatment markedly inhibited inflammatory cell infiltration, synovitis, and bone erosion, which was associated with lower mean histopathological score

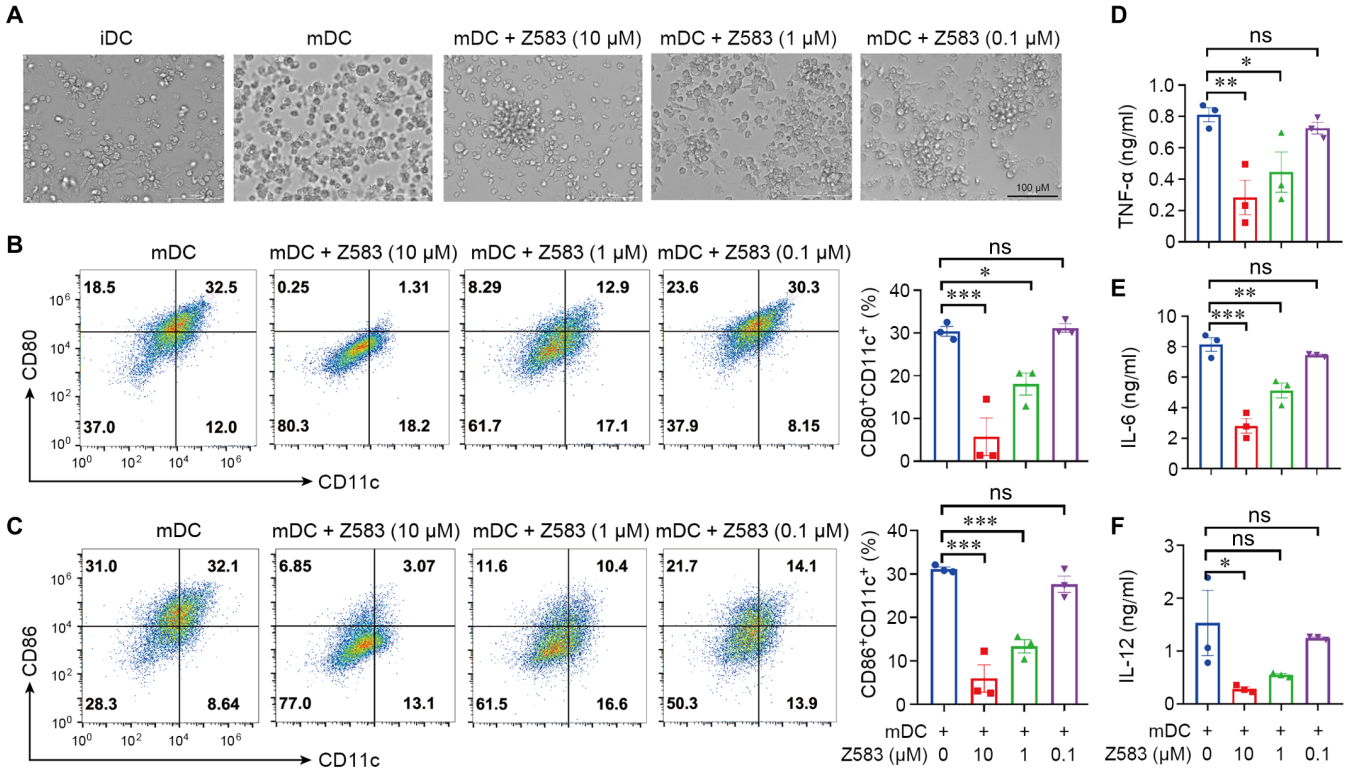

Fig. 4. Z583 inhibited the phenotypic maturation of DCs in vitro. (**A**) Representative morphology of DC population after different treatment as shown by phase-contrast microscopy. iDCs from monocytes of C57BL/6 mice were pretreated with Z583 (10, 1, and 0.1 μM) for 1 hour and then followed by LPS stimulation for another 24 hours; percentage of $CD80^+CD11c^+$ (**B**) and $CD86^+CD11c^+$ (**C**) cells were analyzed by flow cytometry. The production of proinflammatory cytokines TNF-α (**D**), IL-6 (**E**), and IL-12 (**F**) in the supernatant was measured by enzyme-linked immunosorbent assay (ELISA). All data are from three independent experiments. Data are presented as means ± SEM; $^*P < 0.05$, $^{**}P < 0.01$, and $^{***}P < 0.001$ versus LPS-treated control group.

compared to vehicle-treated mice (Fig. 6, F to G). Furthermore, Z583 treatment also alleviated collagen-induced bone and cartilage destruction. Findings from micro-CT imaging were consistent with the histopathologic analysis, which was that the bone destruction in the hindlimb joint was completely abrogated via Z583 treatment (Fig. 6J). As selective JAK3 inhibitors, we compared the efficacy of Z583 and ritlecitinib at the same dose of 10 mg/kg (orally) in a CIA mouse model (fig. S1E). The results demonstrated that they had almost identical therapeutic effects with regard to clinical scores after 2 weeks of treatment, but Z583 had a superior effect in inhibiting arthritis incidence (fig. S1, F and G). In addition, approved pan-JAKinibs of tofacitinib and baricitinib were chosen to compare the efficacy with Z583 for in vivo treatment experience. Our data indicate that tofacitinib and baricitinib also inhibited the development of arthritis in vivo, but Z583 indicated superior preventive effects compared to that of pan-JAKinibs at the same dose (figs. S2 and S3).

Given the strong efficacy of Z583 in preventing the development of arthritis, we hypothesized that Z583 would also be efficacious in reversing paw inflammation and swelling in the CIA model that occurred. To test this hypothesis, we administered Z583 to the CIA mice from day 43 when their paws had already swollen. Treatment with 10 mg/kg dose of Z583 for 4 weeks miraculously reduced the clinical scores compared to that of the vehicle-treated controls (Fig. 6, K and L). Together, Z583 not only prevented the onset and reduced the severity of RA by inhibiting inflammatory cell infiltration and mitigating cartilage and bone erosion but also reversed the inflammatory phenotype of established arthritis.

The safety and pharmacokinetic properties of Z583

To further estimate the druggability and clinical value of Z583, we carried out a preliminary assessment of its safety and metabolism. The acute toxicity profile of Z583 was evaluated via oral administration of a signal dose of Z583 (2 g/kg) in adult Institute of Cancer Research (ICR) mice (n = 10; 5 males and 5 females). After administration of Z583, mice were monitored for abnormal behavior and mortality during the first 4 hours, the next 24 hours, and thereafter for 14 days. During the surveillance period, no acute toxic effects were observed, and the median lethal dose (LD_{50}) of Z583 was found to be >2 g/kg by oral administration (Fig. 7A). Moreover, the possibility of cardiovascular risk was evaluated by a hERG (the human Ether-à-go-go–related gene) potassium channel patch-clamp assay. The Z583 did not show an inhibitory effect on hERG with an IC_{50} value over 30 μM, which indicates a low risk of drug-induced corrected interval of Q-wave to T-wave (QTc) prolongation-associated cardiovascular events (Fig. 7B). The bacterial reverse mutation assay (Ames) was used to evaluate the genetic toxicity of drugs. We found that Z583 was negative in two *Salmonella typhimurium* strains (TA100 and TA102) in the presence and absence of S9 (rat liver microsomal enzyme) mixture, indicating a low mutagenic or carcinogenic potential (Fig. 7C). Next, the subacute toxicity of Z583 was evaluated to broadly understand the safety of Z583 at doses of

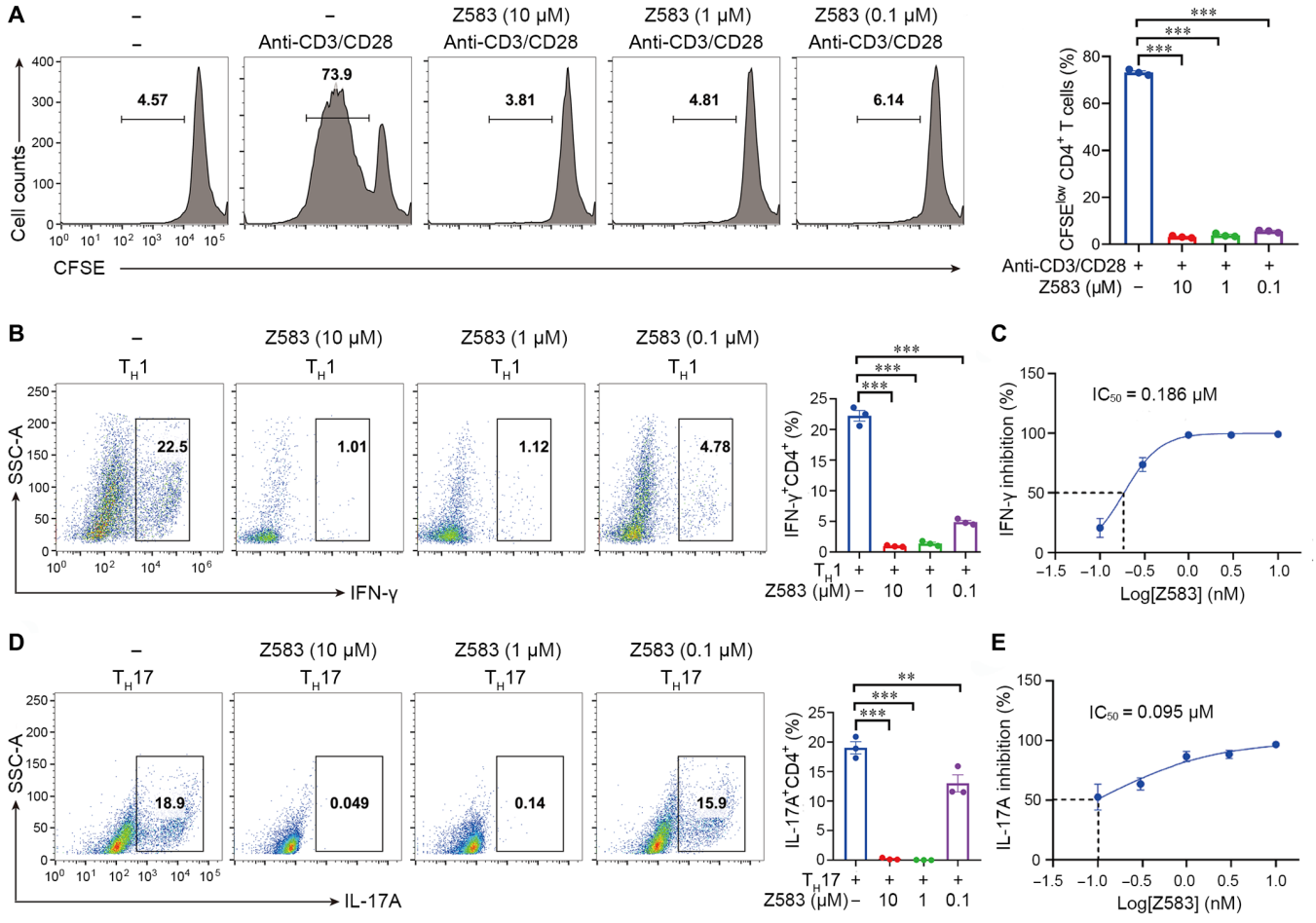

Fig. 5. Selective JAK3 inhibition with Z583 suppressed the naïve T cell proliferation and differentiation. Naïve $CD4^+$ T cells from lymph nodes of C57BC/6 mice were isolated to perform the proliferation and differentiation assays. (**A**) Naïve $CD4^+$ T cells were stimulated with anti-CD3/anti-CD28; the effect of Z583 on T cell proliferation was analyzed by flow cytometry. $CD4^+$ T cells were stimulated with anti-CD3/anti-CD28 in the presence or absence of Z583 (10, 1, and 0.1 μM) for 72 hours; the expression of IFN-γ (**B**) and T_H17A (**D**) was analyzed by flow cytometry. The production of IFN-γ (**C**) and T_H17A (**E**) by $CD4^+$ T cells in the supernatant was measured by ELISA; the IC_{50} values of Z583 (0.01, 0.3, 1, 3, and 10 μM) for inhibiting T cell differentiation were calculated. All data are from three independent experiments. Data are presented as means ± SEM; $^{**}P < 0.01$ and $^{***}P < 0.001$ versus anti-CD3/anti-CD28–treated control group.

20, 60, and 180 mg/kg in rats (n = 10 for each dose; 5 males and 5 females) for four consecutive weeks by oral administration. Biochemical and hematological parameters were tested weekly during the experimental period. These results indicated that Z583 did not have an effect in body weight (fig. S4), general hematological parameters (table S2), or the biochemical parameters of liver and kidney function lipid profiles (table S3) at each time point compared to the control rats. Furthermore, no significant macroscopic and pathological changes were found in the liver, heart, lung, spleen, kidney, testis, and stomach tissues by hematoxylin and eosin (H&E) staining (figs. S5 and S6).

JAK2 contributes to the maturation of erythrocytes via EPO signaling and the formation of platelets by TPO signaling. Therefore, anemia and leukopenia are common adverse events that occur in clinical treatment with pan-JAKinibs. To validate the effects of Z583 on hematopoiesis in vivo, we analyzed the hematopoietic cell numbers in blood from rat that were dosed with Z583 at 20, 60, and 180 mg/kg after four consecutive weeks with oral administration. The results showed that Z583 did not cause a decrease in the total number of white blood cells, including that of monocytes, lymphocytes, and neutrophils (Fig. 7, D to G). These data suggest that selectively inhibiting JAK3 does not have an effect on the survival and proliferation of white blood cells even at the high dose of 180 mg/kg for 4 weeks. In addition, red blood cells, hemoglobin levels, and hematocrit were also not affected by high-dose Z583 (Fig. 7, H to J). The proliferation of platelets was driven by TPO-mediated JAK2 signaling, and aberrant platelet counts could lead to potential thrombotic event. We found that Z583 did not have an effect on platelet formation in the peripheral blood of mice, which is in line with selectivity for JAK3 (Fig. 7K). These data demonstrated that Z583 maintains selectivity over JAK2 in vivo, and long-term administration of Z583 is safe for the hematological system.

To evaluate the pharmacokinetic properties of Z583, a preliminary pharmacokinetic analysis was conducted in mice following intravenous and oral administration. As demonstrated in Fig. 7L, an oral dose of Z583 at 30 mg/kg exhibited a reasonable pharmacokinetic profile with a $t_{1/2}$ of 1.22 hours. The area under the curve [AUC(0 – t)] value is 801.05 μg/l*h, and moderate oral bioavailability (% F) is 24.66%. Furthermore, in vitro absorption, distribution, metabolism,

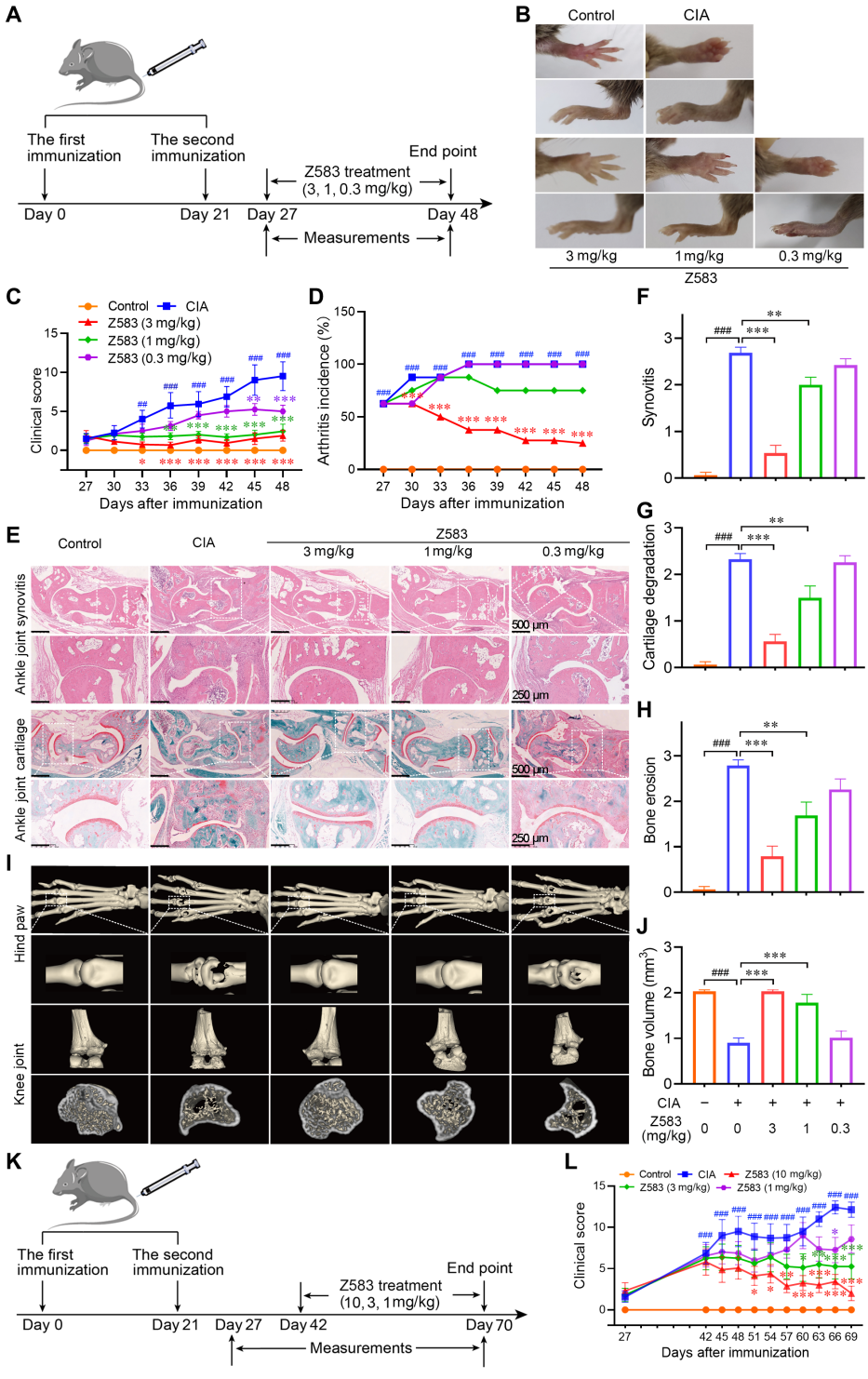

Fig. 6. Selective JAK3 inhibitor Z583 treatment alleviated CIA in mice. (**A**) Experimental scheme of the prophylactic effect of Z583 for the analysis of CIA; DBA/1 mice were immunized on days 0 and 21 and were treated with different doses of Z583 (3, 1, and 0.3 mg/kg) from day 27 for 3 weeks. (**B**) Representative hind paws from each treatment group. Clinical score (**C**) and CIA incidence (**D**) were assessed every 3 days in control, CIA mice, and Z583-treated CIA mice. (**E**) Ankle joint sections were stained by hematoxylin and eosin (H&E) or saffron O/Fast green staining. Quantification of synovitis (**F**), cartilage degradation (**G**), and bone erosion (**H**) in ankle joint was assessed using clinical scores on day 48. (**I**) Representative micro-CT images of hind paws and knees. (**J**) Bone volume of the right hind paw second to fourth metatarsophalangeal joint was assessed using Mimics software. (**K**) Experimental scheme of the therapeutic effect of Z583 for the analysis of CIA. DBA/1 mice were immunized on days 0 and 21 and were treated with different doses of Z583 (10, 3, and 1 mg/kg) from day 43 for 4 weeks. (**L**) Clinical score was observed every 3 days in control, CIA mice, and Z583-treated CIA mice. Data are presented as means ± SEM, $n = 8$. ##$P < 0.01$ and ###$P < 0.001$ versus control group; *$P < 0.05$, **$P < 0.01$, and ***$P < 0.001$ versus CIA group.

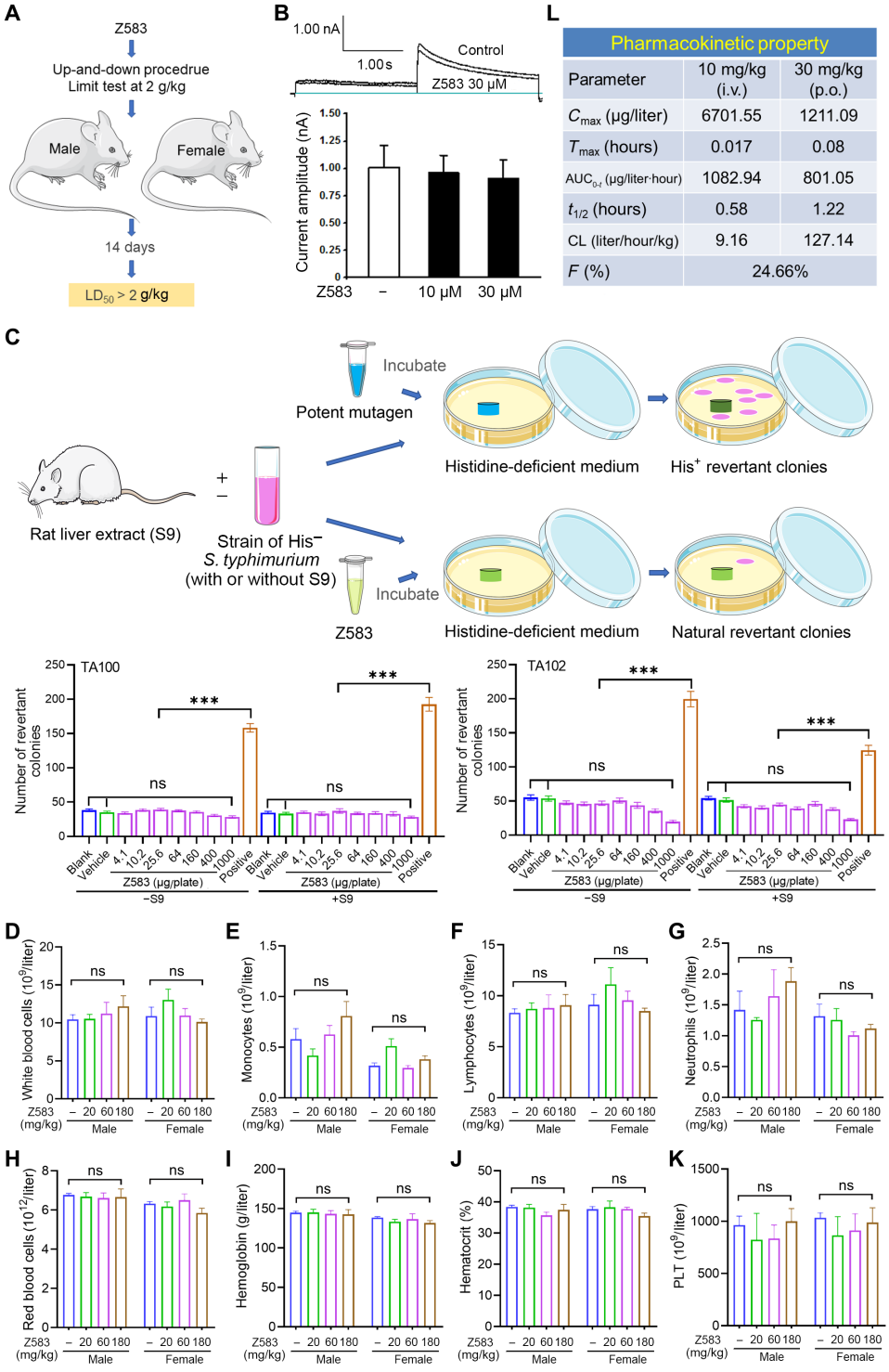

Fig. 7. Safety and pharmacokinetic property of Z583. (**A**) Signal dose acute oral toxicity was performed by up-and-down procedure according to the Organization for Economic Cooperation and Development for chemical testing guidelines no. 425 and limited test with single dose at 2 g/kg. (**B**) Chinese hamster ovary cells were used to measure the possible inhibition of Z583 for hERG potassium current by patch-clamp recording. (**C**) *S. typhimurium* strains TA100 and TA102 were used to evaluate the mutagenic potentials of Z583 by bacterial reverse mutation assay; data are presented as means ± SEM, $n = 3$; ***$P < 0.001$ versus positive control; ns, no statistical significance of positive group versus blank or vehicle group. White blood cells (**D**), monocytes (**E**), lymphocytes (**F**), neutrophils (**G**), red blood cells (**H**), hemoglobin (**I**), hematocrit (**J**), and platelets (**K**) were measured in the blood of rats dosed for 4 weeks with Z583 at 20, 60, and 180 mg/kg ($n = 10$); data are presented as means ± SEM. ns, no statistical significance of control group versus three treatment group. (**L**) Preliminary pharmacokinetic property of Z583 by oral (p.o.) and intravenous (i.v.) route in mice ($n = 8$) was analyzed by LC-MS/MS.

and excretion (ADME) analysis revealed that Z583 has excellent metabolic stabilities against human hepatocytes and human whole blood with $t_{1/2}$ values of 1 and 3.2 hours, respectively (tables S4 and S5). Overall, the selective JAK3 inhibitor Z583 demonstrated a favorable safety profile and drug-like pharmacokinetic properties in vivo and in vitro, which merits further research and development.

DISCUSSION

Cytokine signaling is critical for cellular growth, development and differentiation, immune homeostasis, and host defense (*12*). However, inappropriate and excessive secretion of cytokine is directly associated with the pathogenesis of inflammatory and autoimmune disorders. This has been proven by successful biologic therapeutics of monoclonal antibodies and recombinant proteins that target individual cytokines and their receptors (*16*). Although these biological blockers are a promising alternative therapy for RA, psoriasis, and other autoimmune disease, their clinical application is limited because of the immunogenicity of antibodies and the low efficacy of targeting single cytokines. Therefore, many of these biological drugs do not achieve complete remission or patients are unresponsive to the treatment. Hence, a novel or alternative therapeutic strategy that targets multiple proinflammatory cytokine-dependent signaling pathways needs to be developed for the treatment of autoimmune and inflammatory diseases. Cytokines that bind to type I or type II receptors exert their effects through the JAK-STAT pathway. JAKs are essential signaling mediators that are downstream of many proinflammatory cytokines. The therapeutic effects of approved several JAKinibs have been validated in clinical practices, including for the treatment of RA, IBD, and psoriasis. However, the current pan-JAKinibs (i.e., tofacitinib, baricitinib, and upadacitinib) extensively block multiple cytokines through nonselective inhibition of the different JAK isoforms, which results in severe opportunistic infections, anemia, and other side effects (*28*, *29*). Therefore, to overcome these severe side events and maintain their therapeutic efficacy, the next-generation JAKinibs with greater selectivity for specific JAK subtypes need to be developed. Here, our study focused on the JAK3 subtype to find the new-generation selective JAKinib. To date, no highly selective JAK3 inhibitors have been approved for administration in clinical disease treatment. In addition, several selective JAK3 inhibitors were reported to occur at different research stages (*30*–*32*). JAK3 was chosen as the target to find the selective small-molecule inhibitor because of the following reasons. First, JAK3 is predominantly expressed in hematopoietic cells compared to other three subtype extensive expression (*33*). Second, JAK3 mediates signaling only for the common γc relative cytokines (IL-2, IL-4, IL-7, IL-9, IL-15, and IL-21), compared to other three JAK isoforms (*16*). Third, JAK3 has a unique cysteine residue at position 909, and this residue is replaced by serine in an equivalent position in the other three JAK isoforms (*34*). The above specificity of the JAK3 isoform made it a potentially ideal target to find the selective JAK3 inhibitors. Here, a selective JAK3 inhibitor Z583 was developed with the aim of avoiding adverse events, while maintaining potent efficacy at the same time. Our data demonstrate that Z583 potently inhibited the JAK3 isoform with an IC_{50} value of 10.84 nM (1 mM ATP), with a more than 920-fold high selectivity for JAK3 over the other three JAK subtypes. Z583 also significantly inhibited the activation of JAK3-related cytokine-mediated JAK-STAT signaling pathway, as well as $CD4^+$ T cell differentiation. Further research indicated that Z583 was sufficient to block the development of inflammatory response with a dose of 3 mg/kg by oral administration in the CIA model mice, while sparing hematopoietic function.

With regard to JAKinibs, the important question is that we do not know which JAK isoforms to target that will offer maximum efficacy and optimal side effect profile. Members of JAKs are ubiquitously expressed among virtually all cell types, with the exception of JAK3, which is confined to express in hematopoietic cells, regulating the biological effect of more than 50 cytokines. The extensive cellular expression makes the wide-ranging effect of JAK inhibition for a wide variety of inflammatory and autoimmune diseases (*20*). Therefore, extensive inhibition of cytokine signaling by nonselective JAKinibs may cause abnormalities in their physiological function. The side effects of pan-JAKinibs, especially opportunistic infections, are largely only related to these simultaneously blocking multiple cytokines (*35*). Among the four JAK subtypes, only JAK2 responds to the receptor signaling from EPO, TPO, and GM-CSF cytokine families, which regulate the function of hematopoietic system, including erythropoiesis and myelopoiesis (*21*). Therefore, nonselective inhibition for JAK2 is responsible for adverse effects of anemia and leukopenia. These common side effects that are induced by pan-JAKinibs are theoretically predictable on the basis of their biological functions of different JAK subtypes for the corresponding cytokine families. Compared to the other three JAK subtypes, JAK3 only contributes to regulating the function of γc cytokines (*36*). This should result in a much narrower spectrum of cytokine action for selective JAK3 inhibitor compared to pan-JAKinibs and, concomitantly, to avoid the side effect of infection caused by inhibiting multiple cytokines. If developed potent JAK3 inhibitors simultaneously have high selectivity and do not inhibit the function of JAK2 subtype, then they have the potential to overcome the mainly common adverse effects of infection and anemia induced by pan-JAKinibs. Together, on the basis of the biological function and specific tissue expression of various subtypes of the JAK family, JAK3 has become a potentially ideal target for the treatment of inflammatory and autoimmune diseases. A key challenge in the discovery of selective JAK3 inhibitors is that isoforms of the JAK family have near-identical ATP binding sites and there is >80% homology between them. An important amino acid sequence that differs between JAK3 and other JAK members is a cysteine residue within the ATP binding pocket at 909 site, which is replaced by a serine residue in the other three isoforms (*34*). The cysteine residue has a highly nucleophilic thiol group, which is facilitated to achieve irreversibly covalent binding with electrophilic "warheads" by the Michael addition reaction (*34*). Therefore, targeting the nucleophilic thiol of Cys^{909} to design compounds with electrophilic moiety is a viable strategy to find JAK3 covalent inhibitors, thereby obtaining selectivity to JAK3 over the other JAK subtypes. Acrylamide, with potently electrophilic properties, is often used as covalent warhead to design selective JAK3 kinase inhibitors (*37*). Ritlecitinib has been designed and found as a selective JAK3 inhibitor by this strategy. Notably, our research has designed and identified a selective JAK3 inhibitor, Z583, which shows highly potent inhibition for JAK3 with an IC_{50} value of 0.1 nM (K_m ATP) or 10.84 nM (1 mM ATP) in the biochemical assays. In an in vivo experiment, Z583 obviously did not only completely prevent but also did reverse the inflammatory phenotype in mice with CIA. Although Z583 selectively targets the JAK3 subtype regulating narrow-ranging γc family of cytokines, it did display a sufficient anti-inflammatory effect in vitro and in vivo.

To date, none of the approved JAKinibs, including tofacitinib, baricitinib, upadacitinib, and filgotinib, can be truly selective against a certain subtype of JAKs. Their nonselective inhibition for the JAK family leads to a common problem in clinical practice, which is adverse event of infection, anemia, and thrombosis. The new-generation selective JAK3 inhibitors have been developed with the aim of avoiding side effects due to pan-inhibition of the other JAK subtypes, while maintaining potent efficacy. In this study, we demonstrated that the selectivity of Z583 for JAK3 was >920-fold than the other members of JAK kinase. Given the high selectivity of Z583 for the JAK3 subtype, we can speculate that, on the one hand, it can markedly reduce the immune dysfunction caused by inhibiting multiple cytokines. On the other hand, it can avoid the influence to the hematopoietic system function due to nonselective inhibition of the JAK2 subtype. This also confirmed that there were no changes on hematological parameters via our subacute toxicity assay after 28 consecutive days of oral administration with a dose of 180 mg/kg in the rat. However, highly selective JAK3 inhibitors could also assume that this restricted blockade of only γc cytokines may also have the possibility of reduced efficacy. To test whether selective JAK3 inhibitor Z583 maintains efficacy, two separate in vivo assays were carried out to evaluate its anti-RA effect in mice CIA model. In the classic mice CIA model, a dose of Z583 at 3 mg/kg completely prevented the development of an inflammatory phenotype. In another modified classic mice CIA model, DBA/1 mice were administrated Z583 after the mice's paws had already become swollen. Results indicated that Z583 almost reversed the edematous paws at a dose of 10 mg/kg. Our data demonstrate that Z583 is sufficient to inhibit the development of inflammation and ameliorate RA in a mouse model of CIA. It implies that selective JAK3 subtype inhibition alone is fully capable of maintaining potent efficacy in RA while, at the same time, avoiding adverse events, such as infection and anemia.

As the most efficient antigen-presenting cells, DCs play various roles with regard to coordinating immune response against a threat, regulating the immune system at steady state, and inducing immune tolerance (*38*). In peripheral tissues, DCs exist as immature cells, and inducing tolerance can manipulate different immune cells to suppress autoimmune responses in vivo (*39*). mDCs present antigen to T cells to exert the following effect on the one hand and secrete cytokines to directly regulate the differentiation of naïve T cells on the other hand. In our study, we found that a selective JAK3 inhibitor was able to block the maturation of DCs by inhibiting the expression of CD86 and CD80 while reducing the production of proinflammatory cytokines. These findings demonstrate that DCs play an important role in regulating JAK-STAT signaling of inflammatory and autoimmune diseases. It also implies that γc-related cytokines may be involved in the maturation of DCs. Generally, DCs are essential for differentiation of naïve T cells, which are involved in the progression of inflammatory and autoimmune disease. It is well known that T_H1 and T_H17 subsets drive RA by producing different types of cytokines. The γc cytokines, including IL-2 and IL-21, are among the main cytokines that are produced by T_H1 or T_H17 cells (*40*). They act on diverse target cells to produce immune responses. Here, we determined the effect of the selective JAK3 inhibitor Z583 on differentiation of naïve T cells. Our data demonstrate that Z583 significantly inhibited the T_H1 and T_H17 subset differentiation from naïve $CD4^+$ T cells from the lymph nodes of mice. Furthermore, the result was also validated by an in vivo experiment with or without Z583-treated CIA mice. These results suggest that the efficacy of selective JAK3 inhibitor on RA was implicated in the maturation of DCs and differentiation of naïve T cells.

In summary, the key advantages of selectively acting on the JAK3 subtype to treat inflammatory and autoimmune diseases are that the expression of JAK3 subtype is restricted to the hematopoietic cells and contributes to signals from the γc family of cytokines. Theoretically, this advantage has the potential to avoid any adverse events that are induced by nonselective inhibitors. In addition, it also makes the JAK3 subtype a potential ideal target in comparison to the other members of JAK family. In this study, we found the presence of an irreversibly selective JAK3 inhibitor, Z583, which contains a potent inhibitory effect on JAK3, as well as higher selectivity against other three members of the JAK family. We demonstrated that Z583 could completely inhibit JAK3-regulated γc cytokine signaling and display an amazing therapeutic effect in an animal model of RA. Subacute toxicity test results revealed that highly selective inhibition for JAK3 by Z583 also helped avoid adverse events, such as anemia and hemocytopenia, which is regulated by the JAK2 subtype. Last, our data support that Z583 is a highly selective JAK3 inhibitor, which maintains potent efficacy on RA while avoiding the side effects due to systemic suppression. These results make Z583 an attractive novel candidate for RA and make Z583 worthy of further evaluation in clinical study.

MATERIALS AND METHODS

Experimental design

The objective of this study was to characterize and evaluate the potential of Z583 in preclinical druggability on RA. The binding potency and selectivity of Z583 to the recombinant human kinases of JAK1, JAK2, JAK3, and TYK2 were measured by HTRF KinEASE-TK assay and fluorescence resonance energy transfer (FRET)–based Z′-LYTE assay. The kinome profiling selectivity of Z583 was evaluated using KINOMEscan technology against a panel of 463 kinases. The target engagement and binding mode of Z583 with JAK3 protein was evaluated by a molecular docking study, cell-based washout experiment, and LC-MS/MS analysis. In vitro signaling and functional roles of Z583 for JAK-STAT signaling pathway, T cell proliferation and differentiation, and maturation of DCs were investigated using primary hPBMCs, primary mice bone marrow–derived DCs (BMDCs), and naïve $CD4^+$ T cells by Western blot, flow cytometry, and other assays. The mutagenic potential of Z583 was determined using standard plate incorporation assays with *S. typhimurium* strains TA100 and TA102. Chinese hamster ovary cells were used to assess the inhibition of Z583 on hERG potassium channel by whole-cell patch-clamp recording. For in vitro assays, at least three independent experiments were performed. For in vivo studies, the DBA/1 mice model of RA was used to evaluate the efficacy of Z583 by measuring clinical arthritis score, arthritis incidence, histopathological score of joint, cartilage damage, and bone erosion with blinding. The safety of Z583 was further evaluated via an acute toxicity assay in the ICR mice by determining LD_{50} and subacute toxicity assay in Sprague-Dawley (SD) rats by detecting biochemical and hematological parameters. The pharmacokinetic characteristics of Z583 were carried out using Balb/C mice by analyzing the pharmacokinetic parameters. Animals were randomly assigned to different groups, with at least eight animals per group before initiating the experiment. Animals were examined daily and then humanely euthanized at defined study end points. All animal procedures were carried out

in accordance with the guidelines of the Animal Care and Welfare Committee of the Institute of Materia Medica, Chinese Academy of Medical Sciences and Peking Union Medical College.

Reagents

Z583 was designed and synthesized by Y. Yin and D. Zhang (China Pharmaceutic University, Nanjing, China). The recombinant human kinases JAK1 (pv4774), JAK2 (pv4220), JAK3 (pv3885), and Tyk2 (pv4790) were bought from Invitrogen (Carlsbad, CA, USA). HTRF KinEASE-TK assay kit was purchased from Cisbio Bioassays (Codolet, France). The mouse enzyme-linked immunosorbent assay (ELISA) kits of TNF-α (88-7324-88), IL-6 (88-7064-88), IL-12 (88-7121-88), IFN-γ (88-7314-88), and IL-17A (88-7371-88) were purchased from Invitrogen (Carlsbad, CA, USA). The recombinant human or mouse cytokines involved in the experiments are listed in table S6.

Experimental animals

The C57BL/6 male mice (20 to 22 g, 6 to 8 weeks), DBA/1 male mice (21 to 22 g, 8 to 10 weeks), Balb/C mice (21 to 23 g, 6 to 8 weeks), ICR mice (22 to 25 g, 8 to 10 weeks), and SD rats (180-200 g, 6 weeks) were all purchased from the Beijing HFK Bioscience Co. Ltd. (Beijing, China). Animals were housed five per cage at room temperature of 22° ± 2°C in specific pathogen–free conditions under a 12-hour light/12-hour dark cycle, with food and water provided ad libitum. All animal experimental procedures used in this study were approved by the Animal Care and Use Committee of Institute of Materia Medica, Chinese Academy of Medical Sciences and Peking Union Medical College (approval no. 00005958). The animal study also accorded with the Animal Research: Reporting of In Vivo Experiments (ARRIVE) guidelines.

Biochemical kinase inhibition assay

The in vitro JAKs assays were performed by HTRF KinEASE-TK assay according to the manufacturer's instruction. Briefly, the reaction mixture contains enzyme [JAK1 (1 ng/μl), JAK2 (0.004 ng/μl), JAK3 (0.012 ng/μl), or Tyk2 (1 ng/μl)], 1 μM TK-substrate-biotin, K_m concentration of ATP (4 μM for JAK1, JAK2, and Tyk2 and 1.43 μM for JAK3), or 1 mM ATP in an assay buffer consisting of 20 mM Hepes (pH 7.5), 1 mM dithiothreitol, and 5 mM $MgCl_2$. Compounds were then dissolved into 2% dimethyl sulfoxide (DMSO) with seven concentrations, ranging from 10 μM to 0.01 nM (10-fold dilutions). All reactions were initiated by the addition of ATP and TK-substrate-biotin, incubated at 30°C for 30 min and then quenched with a stop buffer containing 25 nM Strep-XL665 and TK Ab-Cryptate. The plates were then incubated for 1 hour before being read on synergy H1 (BioTek, Winooski, Vermont, USA) using standard HTRF settings. Furthermore, IC_{50} was calculated via a nonlinear regression using the GraphPad Prism 8.0 software.

Kinome scanning assay

The kinome profiling selectivity of Z583 with 100 nM concentration was determined at the Eurofins DiscoverX Corporation in Fremont, CA, USA by applying the KINOMEscan technology against a panel of 463 kinases. The experimental procedures were described in the Supplementary Materials. The selectivity *S* score was used to quantitatively measure the compound selectivity and was calculated using percent control as a potency threshold to describe compound selectivity and to facilitate comparison of different compounds.

FRET-based Z′-LYTE assay

The inhibitory activities of Z583 (100 nM) against kinases were performed using the FRET-based Z′-LYTE assay and LanthaScreen assay according to the manufacturer's instructions (Invitrogen, Carlsbad, CA). Briefly, a mixture of kinases, ATP, and substrate peptide were prepared in a kinase buffer [1 mM EGTA, 10 mM $MgCl_2$, 0.01% BRIJ-35, and 50 mM Hepes (pH 7.5)]. The final 10 μl of kinase reaction solution was composed of 5 μl of peptide/kinase mixture, 2.5 μl of kinase buffer with the test compound, and 2.5 μl of ATP (K_m concentration) solution within the kinase buffer. After 1 hour of incubation at room temperature, 5 μl of the development reagent solution was added for incubation for 1 hour at room temperature, before which 5 μl of the stop solution was added. Last, the fluorescence signal of mixture was assessed using a plate reader.

Molecular modeling

The CDOCKER module of Discovery Studio 2016 was used for molecular docking. Z583 was drawn and then converted into a 3D structure, followed by local minimization using the chemistry at HARvard macromolecular mechanics (CHARMM) force field and was docked to the x-ray crystal of JAK3 (PDB code: 4Z16). The binding site was determined by the initial ligand within the crystal structure. Furthermore, 10 docking poses were calculated for Z583, and the docking poses were ranked according to their -CDOCKER interaction energy and the top pose (-CDOCKER_INTERACTION ENERGY = 48.3355), which was chosen for further analysis. The covalent linkage of Cys^{909} and Z583 was then built manually, and the resulting complex was subjected to energy minimization. The structure was used to analyze the protein-ligand interactions. Last, images were created using PyMOL.

Primary T cell isolation and culture

The naïve $CD4^+$ T cells were isolated from male C57BL/6 mice spleen and lymph nodes and then purified by negative selection using the MojoSort $CD4^+$ Naïve T Cell Isolation Kit (480040, BioLegend). The assays were performed according to the manufacturer's instruction.

Washout experiment

The cultured $CD4^+$ T cells were isolated from C57BL/6 mice and were treated with a series of concentrations of the compound for 1 hour. For the washout groups, cells were gently washed thoroughly with a compound-free complete culture medium three times. This was followed by reincubation of the cells with complete compound-free culture medium. The nonwashout groups were kept in regular culture with compounds. All group cells were stimulated using IL-2 (50 ng/ml; PeproTech) or IL-15 (50 ng/ml; PeproTech) for 30 min. Then, cells were lysed and subjected to a standard Western blot.

LC-MS/MS analysis

The JAK3 protein (10 μg) was labeled with a 10-fold excess of Z583 or DMSO for 2 hours at room temperature. The protein was digested by trypsin using a filter-aided sample preparation method (*41*). The peptide mixtures were then autosampled directly and retained within a C18 reversed-phase column (15 cm in length, 150 μm of inside diameter), which was packed with ReproSil-Pur C18-AQ resin (1.9 μm, 100 Å; Dr. Maisch GmbH, Germany) with a nanoLC UltiMate 3000 system. The sample was separated within a 60-min linear gradient at a flow rate of 600 nl/min. Mobile phase A (99.5% water and 0.5% formic acid) and mobile phase B (80% acetonitrile and 20% 0.1% formic acid in water) were used, with an elution gradient

going from 6 to 9% mobile phase B for 5 min, from 9 to 14% mobile phase B for 15 min, from 14 to 30% mobile phase B for 30 min, from 30 to 40% mobile phase B for 8 min, and from 40 to 95% mobile phase B for 2 min. The nanoLC was directly interfaced using the Q Exactive Hybrid Quadrupole-Orbitrap Mass Spectrometer (Thermo Fisher Scientific). Next, an electrospray voltage of 2.0 kV was used. In MS1, the resolution was 70,000, and the maximum injection time was 20 ms. In MS2, the resolution was 17,500, and the maximum injection time was 60 ms. The raw data files were analyzed and then searched against a target protein database on the basis of species of samples using MaxQuant (1.6.2.10). The search criteria were as follows. First, full tryptic specificity was required. Next, two missed cleavages were allowed. Carbamidomethylation (C) was set as the fixed modifications, and the new modifications were set as the variable modification. The precursor ion mass tolerances were set at 15 parts per million for all MS that were acquired in an orbitrap mass analyzer. The fragment ion mass tolerance was set to 20 millimass units for all MS2 spectra. To confirm labeling sites, an internally calibrated Higher energy Collision induced Dissociation (HCD) spectra [image current detection, resolution at mass/charge ratio (m/z) 400 = 60,000, relative collision energy of 40%] were acquired using an Orbitrap Fusion mass spectrometer (Thermo Fisher Scientific).

Western blot analysis

hPBMCs (iXCells Biotechnologies) were cultured in a RPMI 1640 (Gibco) supplemented with 10% fetal bovine serum (FBS; Gibco), penicillin (100 U/ml), and streptomycin (100 μg/ml) (Life Technologies) at 37°C, 5% CO_2. Purified human $CD34^+$ cells from mobilized blood (iXCells Biotechnologies) were incubated in a X-VIVO 10 medium (Lonza) supplemented with human stem cell factor (40 ng/ml), IL-3 (20 ng/ml), cyclosporin A (1 μg/ml), and 1% antibiotic antimycotic solution (Sigma-Aldrich). Cells were plated in a 24-well plate (5×10^5 cells per well) and treated with Z583 for 1 hour and then stimulated with different recombinant human cytokines (IL-2, IL-4, IL-6, IL-7, IL-9, IL-10, IL-13, IL-15, IL-21, IFN-γ, and GM-CSF for PBMCs and EPO for $CD34^+$ cells). After stimulation, cells were collected and lysed with radioimmunoprecipitation assay buffer [50 mM tris-HCl (pH 7.4), 150 mM NaCl, 1% Triton X-100, 1% sodium deoxycholate, 0.1% SDS, 1 mM sodium orthovanadate, 50 mM NaF, and 50 mM phenylmethylsulfonyl fluoride] along with complete protease inhibitors and phosphatase inhibitors (Cell Signaling Technology, Danvers, MA). Subsequently, protein lysates were quantified using the bicinchoninic acid assay (Thermo Fisher Scientific). Equivalent amounts of total protein were separated by 10% SDS–polyacrylamide gel electrophoresis gel and then transferred to a polyvinylidene difluoride membrane. After blocking, the membrane was incubated with antibodies for STAT1 (1:1000; Cell Signaling Technologies, 14994), p-STAT1 (1:1000; Abcam, ab30645), STAT3 (1:1000; Cell Signaling Technologies, 9139), p-STAT3 (1:1000; Cell Signaling Technologies, 9145), STAT5 (1:1000; Abcam, ab32043), p-STAT5 (1:1000; Cell Signaling Technologies, 4322), STAT6 (1:1000; Abcam, ab44718), p-STAT6 (1:1000; Abcam, ab28829), and glyceraldehyde-3-phosphate dehydrogenase (GAPDH) (1:2000; ZSGB-Bio, China, TA-09), followed by an incubation with a secondary antibody conjugated to horseradish peroxidase (1:2000; ZSGB-Bio, China, ZB-5301). The bands were visualized by using enhanced chemiluminescence reagents from Merck Millipore and then quantified using ImageJ software. Protein expression was normalized against GAPDH.

$CD4^+$ T cell proliferation assays

Purified naïve $CD4^+$ T cells were labeled with carboxyfluorescein succinimidyl amino ester (CFSE; Dojindo, Kumamoto, Japan) according to the manufacturer's instruction. For antigenic stimulation, 2×10^6 CFSE-labeled T cells were incubated with control and compounds for 5 days. The T cells were cultured and then expanded into complete RPMI 1640 with anti-CD3 (100312, BioLegend)/anti-CD28 (102121, BioLegend). The cells were analyzed by flow cytometry at the end of the stimulation period.

$CD4^+$ T cell differentiation

Purified naïve $CD4^+$ T cells were cultured in 96-well plates (2×10^5 cells per well) that were coated with anti-CD3 (1 μg/ml) and anti-CD28 (2 μg/ml) in the presence of compounds or/and cytokines that drive differentiation into T_H1 or T_H17 subsets. For T_H1 cell differentiation, cells were cultured in the presence of anti–IL-4 (10 μg/ml) and IL-12 (10 ng/ml). For T_H17 cell differentiation, a mixture of the following cytokines were used to polarize naïve $CD4^+$ T cells, including anti–IL-4 (10 μg/ml), anti–IFN-γ (10 μg/ml), IL-6 (20 ng/ml), and transforming growth factor–β (10 ng/ml). Compounds were added at different concentrations at the start of T cell polarization to monitor the effect on T cell differentiation. After 5 days, the supernatant was collected to determine IFN-γ (T_H1 marker) or IL-17A (T_H17 marker) by ELISA method, according to the manufacturer's instruction (Invitrogen). Cells were harvested and restimulated with ionomycin (1 μg/ml) and phorbol 12-myristate 13-acetate (20 ng/ml) for 4 hours, blocked with brefeldin A (BioLegend) for 2 hours, and then stained with an anti-CD4 antibody (1:100; BioLegend, 100510). After surface staining, cells were permeabilized with the Foxp3/Transcription Factor Staining Buffer Set (00-5523-00, eBioscience), according to the manufacturer's instructions. In addition, it was stained with anti–IFN-γ (1:100; BioLegend, 505810) or anti–IL-17A (1:100; BioLegend, 506903) antibody to determine T cell differentiation using flow cytometry. Flow cytometry analysis was performed with BD verse and then data were analyzed using FlowJo software.

BMDC culture and cell analysis

The bone marrow cells were flushed out of the mice femur and tibia in phosphate-buffered saline, centrifuged, and then resuspended into an erythrocyte lysis buffer. After incubating for 2 min, the cell suspension was filtered using a 70-μm mesh. The single cells were resuspended into a BMDC culture medium (RPMI 1640) supplemented with 10% FBS, sodium pyruvate, 50 μM 2-mercaptoethanol (Gibco), 10 mM Hepes, penicillin/streptomycin, recombinant mouse GM-CSF (20 ng/ml), and recombinant mouse IL-4 (10 ng/ml). The cells were plated at a density of 5×10^6 cells/ml and then dispensed into 24-well plates. The medium was exchanged on day 3 to remove the free-floating cells, and fresh medium containing suitable reagents was added on day 5. The BMDCs were harvested on day 7, and the supernatant cytokines (i.e., IL-6, TNF-α, and IL-12) were measured by ELISA kits according to the manufacturer's instructions (Invitrogen). The murine BMDCs were immunophenotyped by staining with antibodies against CD11c (1:100; BioLegend, 117310), CD86 (1:100; BioLegend, 105008), and CD80 (1:100; BioLegend, 104706), followed by flow cytometry analysis.

Enzyme-linked immunosorbent assay

The concentration of TNF-α, IL-6, IL-12, IFN-γ, and IL-17A in the culture supernatants were determined by ELISAs according to the manufacturer's instructions.

CIA and treatment protocols

DBA/1 mice were immunized by intradermal injecting with 100 μg of chicken type II collagen solution (Chondrex, Redmond, WA; IMB11) in an equivalent volume of complete Freund's adjuvant (Chondrex, 7001) at the base of the tail, denoted as day 0. On day 21, the mice were immunized again with 50 μg of chicken type II collagen solution in incomplete Freund's adjuvant (Chondrex, 7002). The control mice were injected in a similar manner with saline. Mice with CIA were then divided into four groups (n = 8), including a model group and three Z583-treated groups. From day 27, mice were treated with drugs by oral administration for 3 weeks, and then arthritis disease severity and development in the paws were monitored with clinical arthritis score and arthritis incidence every 3 days. The clinical arthritis score was assessed by grading each paw from 0 to 4 according to the extent of erythema and swelling: 0, normal; 1, slight erythema or swelling of one of the toes or fingers; 2, erythema and swelling of more than one toe or finger; 3, erythema and swelling involved in the ankle or wrist; 4, complete erythema and swelling of toes or fingers and ankle or wrist (*42*). Each limb was graded, and then a mean score was attributed to each animal. To evaluate the real therapeutic effect of Z583, immunized mice were treated with drugs by oral administration from day 42 after the mice's paws had already become swollen for 3 weeks. Arthritis scoring and paw thickness measurements were performed by two independent observers in a blinded manner.

Histopathological analysis

After taking micro-CT, the mice paws were removed from the skin and then decalcified in 5.5% disodium EDTA for 3 weeks. Tissues were then embedded in paraffin, microcosmically sectioned into 5-μm slices, and stained with H&E and saffron O/Fast green. The synovial inflammatory cell infiltration and cartilage degradation were graded on a scale of 0 to 3 based on the severity of joint pathology in five high-power magnification fields as previously described (*43*). The score for every histopathologic feature was calculated in the left hind paw for each animal.

Micro-CT imaging

To evaluate the degree of bone erosion of joints, the paws of mice and ankle joints were fixed in 10% buffered formalin for 48 hours and then scanned in micro-CT (Quantum FX, PerkinElmer). The hind paw scans were performed with 2.5 cm in length, including for an entire single mouse foot with the following parameters: slice increment or thickness of 0.04 mm at 90.00 kV, with a dose of 28,800.00 milliamperes (mAs), with 512 image resolution. The ankle joint scans were performed with 0.51 cm in length including an entire single mouse knee with the following parameters: slice increment or thickness of 0.01 mm at 90.00 kV, with a dose of 28,800.00 mAs, with 512 image resolution. The micro-CT images were imported into a Mimics software (Materialise, Belgium) and then filtered using discrete Gaussian filtering (variance = 1, max kernel width = 1). Volumes of interest in the metatarsophalangeal joint were used to quantify bone erosion as follows. Second to fourth metatarsal and phalangeal bones were segmented using a consistent image intensity threshold. The 3D image of interest was set with ±1 mm in length in the distal and proximal direction from the center of each metatarsophalangeal joint. These volumes of interest were oriented consistently based on the 3D longitudinal axis of the third metatarsal. The bone volumes each of the three metatarsophalangeal joints were calculated.

Acute oral toxicity study

The ICR mice (n = 10; n = 5 male and n = 5 female) were used for the signal dose acute toxicity study by the up-and-down procedure according to the Organization for Economic Cooperation and Development for chemical testing guideline no. 425 for acute oral toxicity testing. In addition, limited test with a single dose of 2 g/kg was performed. Z583 was dissolved into 0.5% Na–*O*-carboxymethylcellulose (CMC) suspensions for oral administration. Once treated with the compound, the mice were monitored for 24 hours for instant death, possible signs of toxicity, and mortality. Then, the mice were observed for an additional 14 consecutive days for any delayed toxic effects. The acute oral toxicity is determined as LD_{50}.

Ames test

The mutagenic potential of Z583 was evaluated with standard plate incorporation assays using *S. typhimurium* strains TA100 and TA102. The compound Z583 was tested with seven doses, ranging from 4.1 to 1000 μg per plate in the absence and presence of metabolic activation (S9). In the test, there were three plates for each dose of compound, solvent control, and positive control groups. The mean value of the revertant frequency was calculated as the average of the duplicate plates in the test. The result was evaluated by the mean number of revertant of the compound compared with vehicle control.

hERG inhibition assay

Chinese hamster ovary cells that express hERG potassium channel were used in the hERG inhibition assay for Z583. Cells were routinely cultured with F-12 medium for 24 hours before being used for the whole-cell patch-clamp recording. Recording pipettes were pulled with a PP-830 patch-pipette puller (Narishige, Tokyo, Japan) and heat-polished to produce about 3 megohm of resistance when filled with pipette solutions. Currents were recorded by PULSE (V8.74, Heka Electronik, Lambrecht, Pfalz, Germany) via an EPC-10 patch-clamp amplifier (Heka Electronik, Lambrecht, Pfalz, Germany), filtered at 2 kHz, and digitized at 10 kHz. Itail was measured at the beginning of the repolarizing pulse, which was indicated as the hERG current. All experiments were conducted at room temperature (22° to 24°C).

Subacute oral toxicity analysis

The SD rats were used to perform the safety of Z583 by 28-day subacute toxicity experiment. Overall, 40 rats were randomly divided into one control group and three experimental groups (n = 10; n = 5 male and n = 5 female). Experimental groups were given Z583 at dosages of 20, 60, and 180 mg/kg by gavage for 28 consecutive days, while the control group was treated with vehicle of solvent. During the experimental period, body weight, food consumption, water intake, abnormal behavior, and any adverse signs of toxicity were observed. At the end of the experiment, all rats were anaesthetized with 4% chloral hydrate, and blood samples were collected for hematological and biochemical analysis. The organs, including the heart, liver, spleen, lung, kidney, testis, ovary, uterine, and stomach, were separated to histopathological analysis.

Hematological analysis

Every week during the experimental period, rats were anesthetized, and the blood samples were collected into tubes containing heparin sodium to detect the total and differential white blood cells, hemoglobin, red blood cell, platelet count, procalcitonin, mean corpuscular hemoglobin, mean corpuscular volume, red blood cell volume,

mean platelet volume, and so on by using an automatic blood cell analyzer (BC-5140 Vet, Mindray, China).

Biochemical analysis

Every week during the experimental period, rats were anaesthetized, and blood samples were collected into nonheparinized tubes and then centrifuged at 3000 rpm at 4°C for 10 min to obtain the serum. The biochemical parameters, including total protein, aspartate aminotransferase, alanine aminotransferase, total protein, albumin, total bilirubin, direct bilirubin, glucose, total cholesterol, triglyceride, low-density lipoprotein, high-density lipoprotein, creatinine, and uric acid, were measured using an automatic biochemical analyzer (7100, Hitachi, Japan). The kits were purchased from Biosino Bio-Technology and Science Inc. (Beijing, China).

Pharmacokinetic study

The male Balb/C mice were used to study the pharmacokinetics of Z583. Overall, 16 mice were randomly divided into an oral administration group (n = 8) and an intravenous administration group (n = 8). Z583 was dissolved in 0.5% Na-CMC suspensions for oral administration (30 mg/kg) and in 0.2% polyoxyethylene castor oil, 0.3% propylene glycol, and 0.3% Tween 80 in saline for intravenous administration (10 mg/kg). Blood samples were collected at different time points (1 min, 3 min, 5 min, 7 min, 10 min, 15 min, 20 min, 30 min, 45 min, 1 hour, 1.5 hours, 2 hours, 2.5 hours, 3 hours, and 4 hours) after oral administration or intravenous injection. Plasma samples were separated by centrifugation of whole blood and stored less than −70°C until bioanalysis. The concentration of Z583 in plasma was detected using LC-MS/MS (Agilent Technologies, 1260 Infinity system). The pharmacokinetic parameters were processed by DAS (version 3.2.8) software.

Statistical analysis

Data were presented as means ± SEM of three or more independent experiments unless stated otherwise. All statistical analyses were performed using GraphPad Prism 8 software (GraphPad Software Inc., La Jolla, CA, USA). The clinical arthritis score was compared using two-factor analysis of variance (ANOVA) followed by Tukey's post hoc test. The other experiments were analysis using one-way ANOVA followed by appropriate post hoc test. $P < 0.05$ was considered statistically significant.

SUPPLEMENTARY MATERIALS

Supplementary material for this article is available at https://science.org/doi/10.1126/sciadv.abo4363

View/request a protocol for this paper from *Bio-protocol*.

REFERENCES AND NOTES

1. N. Bottini, G. S. Firestein, Duality of fibroblast-like synoviocytes in RA: Passive responders and imprinted aggressors. *Nat. Rev. Rheumatol.* **9**, 24–33 (2013).
2. C. Myasoedova, S. Crowson, H. M. Kremers, T. M. Therneau, S. E. Gabriel, Is the incidence of rheumatoid arthritis rising?: Results from Olmsted County, Minnesota, 1955–2007. *Arthritis Rheumatol.* **62**, 1576–1582 (2010).
3. J. S. Smolen, G. Steiner, Therapeutic strategies for rheumatoid arthritis. *Nat. Rev. Drug Discov.* **2**, 473–488 (2003).
4. J. S. Smolen, R. Landewe, J. Bijlsma, G. Burmester, K. Chatzidionysiou, M. Dougados, J. Nam, S. Ramiro, M. Voshaar, R. van Vollenhoven, D. Aletaha, M. Aringer, M. Boers, C. D. Buckley, F. Buttgereit, V. Bykerk, M. Cardiel, B. Combe, M. Cutolo, Y. van Eijk-Hustings, P. Emery, A. Finckh, C. Gabay, J. Gomez-Reino, L. Gossec, J. E. Gottenberg, J. M. W. Hazes, T. Huizinga, M. Jani, D. Karateev, M. Kouloumas, T. Kvien, Z. G. Li, X. Mariette, I. McInnes, E. Mysler, P. Nash, K. Pavelka, G. Poor, C. Richez, P. van Riel, A. Rubbert-Roth, K. Saag, J. da Silva, T. Stamm, T. Takeuchi, R. Westhovens, M. de Wit, D. van der Heijde, EULAR recommendations for the management of rheumatoid arthritis with synthetic and biological disease-modifying antirheumatic drugs: 2016 update. *Ann. Rheum. Dis.* **76**, 960–970 (2017).
5. J. A. Singh, K. G. Saag, S. L. Jr Bridges, E. A. Akl, R. R. Bannuru, M. C. Sullivan, E. Vaysbrot, C. McNaughton, M. Osani, R. H. Shmerling, J. R. Curtis, D. E. Furst, D. Parks, A. Kavanaugh, J. O'Dell, C. King, A. Leong, E. L. Matteson, J. T. Schousboe, B. Drevlow, S. Ginsberg, J. Grober, E. W. S. Clair, E. Tindall, A. S. Miller, T. McAlindon, 2015 American college of rheumatology guideline for the treatment of rheumatoid arthritis. *Arthritis Rheumatol.* **68**, 1–26 (2016).
6. J. S. Smolen, D. Aletaha, I. B. McInnes, Rheumatoid arthritis. *Lancet* **388**, 2023–2038 (2016).
7. S. Siebert, T. Alexander, R. Jamie, M. Iain, Cytokines as therapeutic targets in rheumatoid arthritis and other inflammatory diseases. *Pharmacol. Rev.* **67**, 280–309 (2015).
8. A. Strangfeld, G. R. Burmester, Methotrexate: What are the true risks of treatment? *Ann. Rheum. Dis.* **79**, 1267–1268 (2020).
9. D. H. Solomon, R. J. Glynn, E. W. Karlson, F. Lu, C. Corrigan, J. Colls, C. Xu, J. MacFadyen, M. Barbhaiya, N. Berliner, P. F. Dellaripa, B. M. Everett, A. D. Pradhan, S. P. Hammond, M. Murray, D. A. Rao, S. Ritter, A. Rutherford, J. A. Sparks, J. Stratton, D. H. Suh, S. K. Tedeschi, K. M. M. Vanni, N. P. Paynter, P. M. Ridker, Adverse effects of low-dose methotrexate: A randomized trial. *Ann. Intern. Med.* **172**, 369–380 (2020).
10. D. P. McLornan, J. E. Pope, J. Gotlib, C. N. Harrison, Current and future status of JAK inhibitors. *Lancet* **398**, 803–816 (2021).
11. S. Banerjee, A. Biehl, M. Gadina, S. Hasni, D. M. Schwartz, JAK-STAT signaling as a target for inflammatory and autoimmune diseases: Current and future prospects. *Drugs* **77**, 521–546 (2017).
12. J. J. O'Shea, S. M. Holland, L. M. Staudt, JAKs and STATs in immunity, immunodeficiency, and cancer. *N. Engl. J. Med.* **368**, 161–170 (2013).
13. A. Alunno, I. Padjen, A. Fanouriakis, D. T. Boumpas, Pathogenic and therapeutic relevance of JAK/STAT signaling in systemic lupus erythematosus: Integration of distinct inflammatory pathways and the prospect of their inhibition with an oral agent. *Cell* **8**, 898 (2019).
14. G. L. Goll, T. K. Kvien, New-generation JAK inhibitors: How selective can they be? *Lancet* **391**, 2477–2478 (2018).
15. D. M. Schwartz, Y. Kanno, A. Villarino, M. Ward, M. Gadina, J. J. O'Shea, JAK inhibition as a therapeutic strategy for immune and inflammatory diseases. *Nat. Rev. Drug Discov.* **16**, 843–862 (2017).
16. D. M. Schwartz, M. Bonelli, M. Gadina, J. J. O'Shea, Type I/II cytokines, JAKs, and new strategies for treating autoimmune diseases. *Nat. Rev. Rheumatol.* **12**, 25–36 (2016).
17. P. Macchi, A. Villa, S. Giliani, M. G. Sacco, A. Frattini, F. Porta, A. G. Ugazio, J. A. Johnston, F. Candotti, J. J. O'Sheai, P. Vezzoni, L. D. Notarangelo, Mutations of Jak-3 gene in patients with autosomal severe combined immune deficiency (SCID). *Nature* **377**, 65–68 (1995).
18. Y. Minegishi, M. Saito, T. Morio, K. Watanabe, K. Agematsu, S. Tsuchiya, H. Takada, T. Hara, N. Kawamura, T. Ariga, H. Kaneko, N. Kondo, I. Tsuge, A. Yachie, Y. Sakiyama, T. Iwata, F. Bessho, T. Ohishi, K. Joh, K. Imai, K. Kogawa, M. Shinohara, M. Fujieda, H. Wakiguchi, S. Pasic, M. Abinun, H. D. Ochs, E. D. Renner, A. Jansson, B. H. Belohradsky, A. Metin, N. Shimizu, S. Mizutani, T. Miyawaki, S. Nonoyama, H. Karasuyama, Human tyrosine kinase 2 deficiency reveals its requisite roles in multiple cytokine signals involved in innate and acquired immunity. *Immunity* **25**, 745–755 (2006).
19. P. F. Xu, P. Shen, B. Yu, X. Xu, R. L. Ge, X. Y. Cheng, Q. Y. Chen, J. L. Bian, Z. Y. Li, J. B. Wang, Janus kinases (JAKs): The efficient therapeutic targets for autoimmune diseases and myeloproliferative disorders. *Eur. J. Med. Chem.* **192**, 112155 (2020).
20. M. Gadina, C. Johnson, D. Schwartz, M. Bonelli, S. Hasni, Y. Kanno, P. Changelian, A. Laurence, J. J. O'Shea, Translational and clinical advances in JAK-STAT biology: The present and future of jakinibs. *J. Leukoc. Biol.* **104**, 499–514 (2018).
21. A. L. Basquiera, N. W. Soria, R. Ryser, M. Salguero, B. Moiraghi, F. Sackmann, A. G. Sturich, A. Borello, A. Berretta, M. Bonafé, J. M. Barral, E. D. Palazzo, J. J. García, Clinical significance of V617F mutation of the JAK2 gene in patients with chronic myeloproliferative disorders. *Hematology* **14**, 323–330 (2009).
22. J. M. Parmentier, J. Voss, C. Graff, A. Schwartz, M. Argiriadi, M. Friedman, H. S. Camp, R. J. Padley, J. S. George, D. Hyland, M. Rosebraugh, N. Wishart, L. Olson, A. J. Long, In vitro and in vivo characterization of the JAK1 selectivity of upadacitinib (ABT-494). *BMC Rheumatol.* **2**, 23 (2018).
23. C. J. Menet, S. R. Fletcher, G. Van Lommen, R. Geney, J. Blanc, K. Smits, N. Jouannigot, P. Deprez, E. M. van der Aar, P. Clement-Lacroix, L. Lepescheux, R. Galien, B. Vayssiere, L. Nelles, T. Christophe, R. Brys, M. Uhring, F. Ciesielski, L. Van Rompaey, Triazolopyridines as selective JAK1 inhibitors: From hit identification to GLPG0634. *J. Med. Chem.* **57**, 9323–9342 (2014).
24. J. B. Telliez, M. E. Dowty, L. Wang, J. Jussif, T. Lin, L. Li, E. Moy, P. Balbo, W. Li, Y. Zhao, K. Crouse, C. Dickinson, P. Symanowicz, M. Hegen, M. E. Banker, F. Vincent, R. Unwalla, S. Liang, A. M. Gilbert, M. F. Brown, M. Hayward, J. Montgomery, X. Yang, J. Bauman,

J. I. Trujillo, A. Casimiro-Garcia, F. F. Vajdos, L. Leung, K. F. Geoghegan, A. Quazi, D. Xuan, L. Jones, E. Hett, K. Wright, J. D. Clark, A. Thorarensen, Discovery a JAK3-selective inhibitor: Functional differentiation of JAK3-selective inhibition over pan-JAK or JAK1-selective inhibition. *ACS Chem. Biol.* **11**, 3442–3451 (2016).
25. H. Xu, M. I. Jesson, U. I. Seneviratne, T. H. Lin, M. N. Sharif, L. Xue, C. Nguyen, R. A. Everley, J. I. Trujillo, D. S. Johnson, G. R. Point, A. Thorarensen, I. Kilty, J. B. Telliez, PF-06651600, a dual JAK3/TEC family kinase inhibitor. *ACS Chem. Biol.* **14**, 1235–1242 (2019).
26. R. Nurieva, X. O. Yang, G. Martinez, Y. Zhang, A. D. Panopoulos, L. Ma, K. Schluns, Q. Tian, S. S. Watowich, A. M. Jetten, C. Dong, Essential autocrine regulation by IL-21 in the generation of inflammatory T cells. *Nature* **448**, 480–483 (2007).
27. O. Boyman, J. Sprent, The role of interleukin-2 during homeostasis and activation of the immune system. *Nat. Rev. Immunol.* **12**, 180–190 (2012).
28. S. Cohen, S. C. Radominski, J. J. Gomez-Reino, L. Wang, S. Krishnaswami, S. P. Wood, K. Soma, C. I. Nduaka, K. Kwok, H. Valdez, B. Benda, R. Riese, Analysis of infections and all-cause mortality in phase II, phase III, and long-term extension studies of tofacitinib in patients with rheumatoid arthritis. *Arthritis Rheumatol.* **66**, 2924–2937 (2014).
29. E. C. Keystone, M. C. Genovese, D. E. Schlichting, I. de la Torre, S. D. Beattie, T. P. Rooney, P. C. Taylor, Safety and efficacy of baricitinib through 128 weeks in an open-label, longterm extension study in patients with rheumatoid arthritis. *J. Rheumatol.* **45**, 14–21 (2018).
30. L. Tan, K. Akahane, R. McNally, K. M. S. E. Reyskens, S. B. Ficarro, S. Liu, G. S. Herter-Sprie, S. Koyama, M. J. Pattison, K. Labella, L. Johannessen, E. A. Akbay, K. K. Wong, D. A. Frank, J. A. Marto, T. A. Look, J. S. C. Arthur, M. J. Eck, N. S. Gray, Development of selective covalent Janus kinase 3 inhibitors. *J. Med. Chem.* **58**, 6589–6606 (2015).
31. A. Thorarensen, M. E. Dowty, M. E. Banker, B. Juba, J. Jussif, T. Lin, F. Vincent, R. M. Czerwinski, A. Casimiro-Garcia, R. Unwalla, J. I. Trujillo, S. Liang, P. Balbo, Y. Che, A. M. Gilbert, M. F. Brown, M. Hayward, J. Montgomery, L. Leung, X. Yang, S. Soucy, M. Hegen, J. Coe, J. Langille, F. Vajdos, J. Chrencik, J. B. Telliez, Design of a Janus kinase 3 (JAK3) specific inhibitor 1-((2*S*,5*R*)-5-((7*H*-pyrrolo[2,3-*d*]pyrimidin-4-yl)amino)-2-methylpiperidin-1-yl)prop-2-en-1-one (PF-06651600) allowing for the interrogation of JAK3 signaling in humans. *J. Med. Chem.* **60**, 1971–1993 (2017).
32. L. Y. Shi, Z. P. Zhong, X. T. Li, Y. Q. Zhou, Z. Y. Pan, Discovery of an orally available Janus kinase 3 selective covalent inhibitor. *J. Med. Chem.* **62**, 1054–1066 (2019).
33. M. Kawamura, D. W. McVicar, J. A. Johnston, T. B. Blake, Y. Q. Chen, B. K. Lal, A. R. Lloyd, D. J. Kelvin, J. E. Staples, J. R. Ortaldo, Molecular cloning of L-JAK, a Janus family protein-tyrosine kinase expressed in natural killer cells and activated leukocytes. *Proc. Natl. Acad. Sci. U.S.A.* **91**, 6374–6378 (1994).
34. Q. Liu, Y. Sabnis, Z. Zhao, T. Zhang, S. J. Buhrlage, L. H. Jones, N. S. Gray, Developing irreversible inhibitors of the protein kinase cysteinome. *Chem. Biol.* **20**, 146–159 (2013).
35. K. L. Winthrop, The emerging safety profile of JAK inhibitors in rheumatic disease. *Nat. Rev. Rheumatol.* **13**, 234–243 (2017).
36. R. Roskoski Jr., Janus kinase (JAK) inhibitors in the treatment of inflammatory and neoplastic diseases. *Pharmacol. Res.* **111**, 784–803 (2016).
37. F. Sutanto, M. Konstantinidou, A. Dömling, Covalent inhibitors: A rational approach to drug discovery. *RSC Med. Chem.* **11**, 876–884 (2020).
38. J. Banchereau, F. Briere, C. Caux, J. Davoust, S. Lebecque, Y. J. Liu, B. Pulendran, K. Palucka, Immunobiology of dendritic cells. *Annu. Rev. Immunol.* **18**, 767–811 (2000).
39. S. Khan, J. D. Greenberg, N. Bhardwaj, Dendritic cells as targets for therapy in rheumatoid arthritis. *Nat. Rev. Rheumatol.* **5**, 566–571 (2009).
40. Y. Rochman, R. Spolski, W. J. Leonard, New insights into the regulation of T cells by γc family cytokines. *Nat. Rev. Immunol.* **9**, 480–490 (2009).
41. J. R. Wiśniewski, A. Zougman, N. Nagaraj, M. Mann, Universal sample preparation method for proteome analysis. *Nat. Methods* **6**, 359–362 (2009).
42. M. Miyoshi, S. Liu, Collagen-induced arthritis models. *Methods Mol. Biol.* **1868**, 3–7 (2018).
43. M. Brenner, H. C. Meng, N. C. Yarlett, M. M. Griffiths, E. F. Remmers, R. L. Wilder, P. S. Gulko, The non–major histocompatibility complex quantitative trait locus Cia10 contains a major arthritis gene and regulates disease severity, pannus formation, and joint damage. *Arthritis Rheum.* **52**, 322–332 (2005).

Acknowledgments: We thank G.-Y. Zhu from Macau University of Science and Technology for help with technology of the pharmacokinetic study. **Funding:** This work was supported by National Key R&D Program of China (no. 2020YFA0908004), the National Natural Science Foundation of China (nos. 81973338 and 82104189), CAMS Innovation Fund for Medical Science of China (no. 2017-I2M-3-011), and Fundamental Research Funds for the Central Universities of China (no. 3332020043). **Author contributions:** T.Z., L.S., and D.Z. conceived the idea and designed the research project. C.C., Y.Y., and G.S. fabricated the materials, performed the experiments, and /or analyzed results. C.C., Y.Z., S.S., Y.W., and L.W. analyzed the data and prepared the figures. C.C. and T.Z. wrote the manuscript. T.Z. and L.S. reviewed and revised the manuscript. **Competing interests:** The authors declare that they have no competing interests. **Data and materials availability:** All data needed to evaluate the conclusions in the paper are present in the paper and/or the Supplementary Materials.

Submitted 3 February 2022
Accepted 7 July 2022
Published 19 August 2022
10.1126/sciadv.abo4363